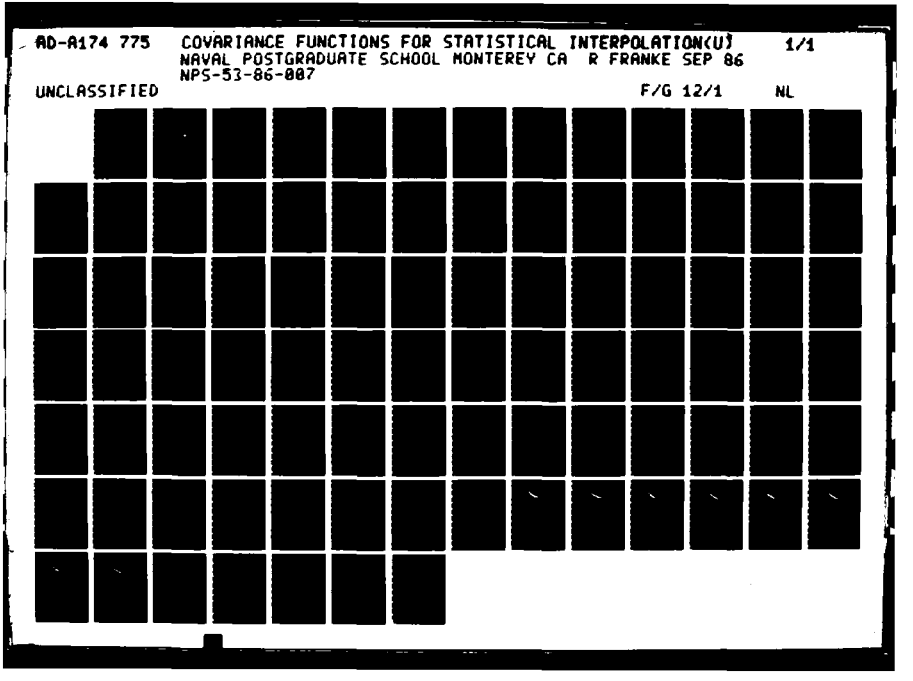
AD-A174 775 COVARIANCE FUNCTIONS FOR STATISTICAL INTERPOLATION(U) 1/1
NAVAL POSTGRADUATE SCHOOL MONTEREY CA R FRANKE SEP 86
NPS-53-86-007
UNCLASSIFIED F/G 12/1 NL

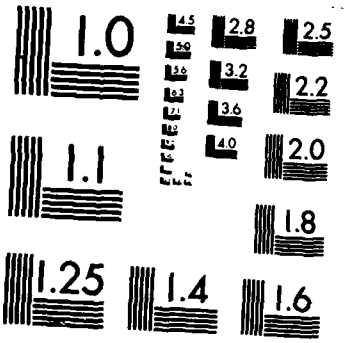

CROCOPY RESOLUTION TEST CHART
NATIONAL BUREAU OF STANDARDS-1963-A

(2)

NPS-53-86-007

NAVAL POSTGRADUATE SCHOOL

Monterey, California

COVARIANCE FUNCTIONS
FOR STATISTICAL INTERPOLATION

by

Richard Franke

September 1986

Technical Report For Period

July 1985 - September 1986

Approved for public release; distribution unlimited

Prepared for:
Naval Environmental Prediction Research Facility
Monterey, CA 93943

NAVAL POSTGRADUATE SCHOOL
MONTEREY CALIFORNIA 93943

R. C. AUSTIN
Rear Admiral, U.S. Navy
Superintendent

D. A. SCHRADY
Provost

This work was funded by the Naval Environmental Prediction Research Facility, Monterey, CA under Program Element 61153N, "Interpolation of Scattered Meteorological Data".

RICHARD FRANKE
Professor of Mathematics

Reviewed by:

HAROLD M. FREDRICKSEN
Chairman
Department of Mathematics

Released by:

KNEALE T. MARSHALL
Dean of Information and
Policy Sciences

UNCLASSIFIED

SECURITY CLASSIFICATION OF THIS PAGE (When Data Entered)

REPORT DOCUMENTATION PAGE		READ INSTRUCTIONS BEFORE COMPLETING FORM
1. REPORT NUMBER NPS-53-86-007	2. GOVT ACCESSION NO. ADA174775	3. RECIPIENT'S CATALOG NUMBER
4. TITLE (and Subtitle) Covariance Functions for Statistical Interpolation		5. TYPE OF REPORT & PERIOD COVERED Technical Report 7/85 - 09/86 6. PERFORMING ORG. REPORT NUMBER
7. AUTHOR(s) Richard Franke		8. CONTRACT OR GRANT NUMBER(s)
9. PERFORMING ORGANIZATION NAME AND ADDRESS Naval Postgraduate School Monterey, CA 93943		10. PROGRAM ELEMENT, PROJECT, TASK AREA & WORK UNIT NUMBERS Program Element 61153N
11. CONTROLLING OFFICE NAME AND ADDRESS Naval Environmental Prediction Research Facility, Monterey, CA 93943		12. REPORT DATE September 1986 13. NUMBER OF PAGES 84
14. MONITORING AGENCY NAME & ADDRESS(if different from Controlling Office) Office of Naval Research Arlington, VA 22217		15. SECURITY CLASS. (of this report) Unclassified 15a. DECLASSIFICATION/DOWNGRADING SCHEDULE

16. DISTRIBUTION STATEMENT (of this Report)

Approved for public release; distribution unlimited

17. DISTRIBUTION STATEMENT (of the abstract entered in Block 20, if different from Report)

18. SUPPLEMENTARY NOTES

19. KEY WORDS (Continue on reverse side if necessary and identify by block number)

objective analysis, parameter estimation, optimum interpolation, isotropic covariance functions, statistical interpolation, covariance functions, data fitting, positive definite functions.

20. ABSTRACT (Continue on reverse side if necessary and identify by block number)

The properties of correlation functions (which are special cases of positive definite functions) are developed. The multivariate application of statistical interpolation in the context of objective analysis of meteorological fields is discussed. Conditions for a one dimensional correlation function to be an isotropic two dimensional correlation function are derived, and a sufficient condition applied to some examples of practical interest. Some

DD FORM 1 JAN 73 1473 EDITION OF 1 NOV 65 IS OBSOLETE

S/N 0102-LF-014-6601

UNCLASSIFIED

SECURITY CLASSIFICATION OF THIS PAGE (When Data Entered)

BLOCK 20

experiments comparing the accuracy of statistical interpolation are reported. The model correlation was a six term Bessel function fit to published data. Functions for several other classes of functions were fit to the same data and their performance compared with the optimum. One appendix gives a compendium of proposed covariance functions, and another reports some experiments concerning estimation of correlation functions from (simulated) raw data.

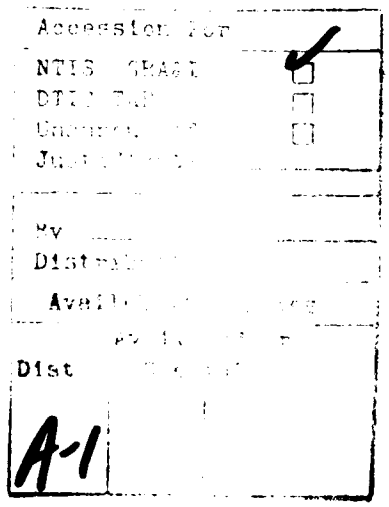

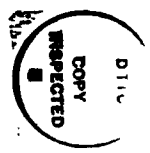

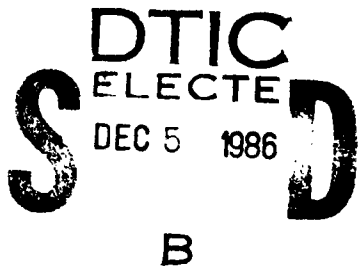

1.0 Introduction

The objective analysis of meteorological data is increasingly being performed by methods based on "Optimum Interpolation", or OI. OI is a statistical scheme with its roots in the ideas of Weiner and Kolmogorov and was introduced to the meteorological literature by Gandin (1963). At about the same time the ideas were also being developed independently in other scientific fields, including geophysics, mining, and electrical engineering. The theoretical basis of OI requires its application to a stationary random field with known statistical properties (for our purposes this is for an ensemble average taken over time), in particular the spatial mean and covariance function are assumed to be known. In addition, errors in the measurements of the field (observations) are assumed to be made with known standard deviation. In meteorology it is usually assumed that the field has zero mean, although this is not strictly required, and as part of the process the mean can be estimated along with the field values.

In meteorology, the process generally proceeds along the following lines for the univariate case. The field to be approximated is the deviation of a first-guess field (e.g., pressure heights) from the true value of the field. The first-guess field can be obtained from climatology, but in current practice is usually the predicted value from a numerical weather prediction model. The first-guess errors are obtained by subtracting the first-guess from the observed values. First-guess values are typically known on a regularly spaced grid, and these values are

interpolated to the irregularly spaced observation points. The interpolation of first-guess errors from the observation points to the grid points is where the application of OI is carried out. Current applications are usually in a multivariate setting, taking into account the physical relationship between meteorological variables such as winds and pressure heights. This requires that cross covariance functions be known or that functional relationships between the variables be assumed.

The practical application of OI requires a great many compromises, so the actual process is usually referred to as statistical interpolation (SI). Some papers dealing with the practical problems are those of Rutherford (1972), Bergman (1979), and Lorenc (1981). The first compromise to be faced is that of estimating the spatial covariance function for the first-guess errors. In practice the covariance function is estimated from historical data (an iterative process, since improved estimates will change the first-guess errors) and is sometimes assumed to be isotropic although, as will be noted later, some gains are apparently obtained by the assumption of anisotropy. The assumption of stationarity is certainly not satisfied and as a practical matter is not necessarily followed. Since the method requires the solution of a system of linear equations in as many unknowns as there are observations, it is necessary to select a subset of the observations to be used for obtaining the first-guess error at a particular grid point (or set of grid points).

The most important problem in the entire process is probably the estimation of the spatial covariance function for the first-guess error field. This problem has been addressed by numerous authors, and has resulted in a great many proposed functional representations. Some of these are listed in Appendix A, using a standardized notation, with references to some of their appearances in the literature. In the past, one commonly used covariance function is the Gaussian, or negative squared exponential. While this function has been used in practice (see Bergman (1979) and Lorenc (1981)), it has also been known for some time that the function has inadequate spectral characteristics (see Julian and Thiébaux (1975)). Another problem is its limited number of parameters, making it difficult to accurately fit the forecast error statistics.

While it has been recognized for many years that the covariance function must be a positive definite function, this has not always been adhered to in practice. One of the advantages of OI is that an estimate of the mean-squared error is easily obtainable, and much is made of this fact. The error estimate is used in quality control as well as to assess the effect of loss of observations on the accuracy of objective analyses (e.g. see Thiébaux, 1980). The error estimates are much more sensitive to mis-specification of parameters than the actual analyses (see Franke, 1985), and the use of nonpositive definite "covariance" functions will undoubtedly cause additional error. Recent emphasis on the necessity of positive definite functions has begun to

make an impact and conditions to guarantee the property can be found in Section 2 of this report.

One class of positive definite functions proposed in the last ten to fifteen years is the class from the covariance functions of autoregressive models, mainly those of order two and three (see Thiébaux, 1976, 1985). These covariance functions arise from random processes which are governed by certain difference equations with random forcing. The underlying process being modeled may or may not be representative of weather processes, but the resulting spatial covariance functions have enough parameters to model the raw statistics to a reasonable degree. The use of these models in anisotropic (product type) and isotropic models has been investigated by Thiébaux (1976, 1985). The use of the one dimensional functions as isotropic multidimensional covariance functions can violate the positive definite condition, however, as is shown in Section 3.

Another class of covariance functions, in use at The European Center for Medium Range Weather Forecasting (originally proposed by Rutherford (1972), and later discussed by Lonnberg (1982) and others) is the Bessel function model. As will be discussed later, a convex combination of Bessel functions $J_0(k_i s)$ and a constant will automatically be positive definite and will allow sufficient parameters to model the forecast error statistics very well. Compared to the autoregressive models, these functions require considerably more computation for their evaluation.

At the present time there is a great deal known about what kinds of functions are suitable for use as multivariate covariance functions, necessary conditions for positive definiteness, and families of such functions which embody enough parameters to allow fitting the forecast error statistics sufficiently well without resorting to functions which are unwieldy for computing. One of the purposes of this report is to attempt to bring together in one place the information in a form accessible to practitioners in the field.

The class of positive definite functions, characterizations of them, and construction of such functions are discussed in Section 2. In Section 3 the general multivariate case are addressed, including conditions for positive definiteness as well as smoothness conditions required when the meteorological variables are related through differentiation. Use of isotropic covariance functions for the multidimensional case, conditions for single dimensional positive definite functions to be isotropic multidimensional positive definite functions, examples and counterexamples are also discussed. In section 4 construction of possible candidates for use as covariance functions is discussed and the results of some estimated rms error calculations under various conditions is given. A listing of functions which have been proposed in the literature as covariance functions is given in Appendix A, and some simulations conducted on estimation of the covariance function from the raw forecast error statistics is given in Appendix B.

2.0 Positive Definite Functions

Covariance functions are positive semi-definite, and thus their theory is closely allied with that of positive definite functions. The purpose of this section is to summarize some of what is known about positive definite functions, and point out properties that are of use in the present context. The discussion will be confined to real functions. An excellent reference for the topic is Stewart (1976).

A function C(s) is said to be positive definite if for any points $s_1, s_2, \ldots, s_n$, and any values $t_1, t_2, \ldots, t_n$, then

$$\sum_{i,j=1}^{n} C(s_i - s_j) t_i t_j \geq 0 \quad .$$

This condition is actually only positive semi-definite, but to distinguish between the two requires excluding certain sets $\{s_i\}$ and $\{t_i\}$, and the possibility of equality in the expression. The additional complication does not add to the theory for the purposes here. An equivalent condition for continuous C(s) is that for all integrable g(s) with finite support,

$$\int_{-\infty}^{\infty}\int_{-\infty}^{\infty} C(s-t)\, g(s)\, g(t)\, ds\, dt \geq 0 \quad .$$

The class of positive definite (PD) functions have some useful properties which will be given and discussed. In what follows, C(s) will denote a PD function.

(1) C(s) is an even function, and this in turn implies that the Fourier transform is the Fourier Cosine transform. This permits the simplification of characterizing PD functions in terms of their Fourier transforms. Additionally, it will be

useful to assume that the argument is always nonnegative to avoid having to indicate absolute values.

(2) The magnitude of C(s) is bounded by its value at the origin. This property is primarily useful to detect that a function is not PD.

(3) A linear combination (with positive coefficients) of PD functions is PD. This makes it easy to construct PD functions with parameters, although when fitting these functions to data one must look at the results to see whether the coefficients obtained are positive.

(4) A product of PD functions is PD. This property is also an aid in constructing PD functions with parameters using simple PD functions as building blocks.

Positive definite functions are characterized by the following property

Theorem: C(s) is PD if and only if the Fourier transform of C is nonnegative.

Thus, PD functions are the (inverse) Fourier transforms of probability density functions (Bochner's Theorem, see Priestly (v.1, 1981)), and since the Fourier transform is the Fourier Cosine transform, the inverse transform and the transform differ only by a constant. The Fourier transform of a probability density function is called a characteristic function.

There are several other properties that are sufficient conditions for a function to be PD.

(1) Laplace transforms of probability density functions are PD. This follows easily from the characterization and an interchange of the order of integration in the Laplace and Fourier transforms.

(2) Convolutions of functions with themselves are PD, i.e.

$$C(s) = \int_0^\infty g(t)\, g(t+s)\, dt \quad \text{is PD.}$$

(3) If $C(s)$ is convex on $(0, \infty)$ and $\lim_{x \to \infty} C(s) = 0$, then $C(s)$ is PD. Unfortunately, this nice condition is not useful, since it will be seen in the next section that covariance functions useful for multivariate statistical interpolation can not be convex.

For illustrative purposes, and to point out some examples that will be useful later on, we note that the following functions are positive definite: e^{-cs}, e^{-cs^2}, $(1 + cs)e^{-cs}$, $\cos(as)$, 1, and $J_0(as)$. The following are not positive definite, although some of them do not seem to be significantly different than the former: $(s^4 + 1)^{-1}$, e^{-as^3}, and $f(s) = 1$ for $0 \leq s \leq 1$, $f(s) = 0$ for $s > 1$.

The above examples can easily be seen to be PD or not by inspection of the Fourier transforms. Because the constant function is PD, its use as a (positive) additive term in modeling covariance functions can be useful over a given spatial range. It must, however, not be truncated at some fixed distance (less than that which might occur in practice) since the resultant function is not PD. Additionally, the above functions are

considered only as functions of one spatial variable. As functions of several spatial variables, the same characterizations hold, although functions which have a positive Fourier transform in one dimension may not have positive transforms in more than one dimension, when considered as isotropic functions, i.e., functions of "distance". Since questions of this sort are closely tied into the problem at hand, their discussion is deferred to Section 3.

3.0 Multivariate Covariance Functions

3.1 General Development

The development of the equations for multivariate application of OI to related variables is discussed in several papers, including Schlatter, et. al. (1976), Bergman (1979), Lorenc (1981), Thiébaux (1985), and Pedder and Thiébaux (1985). At first glance the results do not always seem to be the same, however this is primarily due to different notation being used in such a way as to be potentially confusing.

For completeness, the derivation of the relationship between the covariance functions and cross-covariance functions for variables related through differentiation will be derived here, and the differences with other notations in use noted. Suppose that it is wished to analyze three related dependent variables, requiring that the corrections obtained via OI (or more correctly, SI) will not upset the relationship between the predicted values of the variables. Let the error in the predicted variables be denoted by $Z(x,y)$, $X(x,y)$, and $Y(x,y)$, where (x,y) gives the spatial location and it is assumed that $X(x,y) = k_1 Z_x(x,y)$ and $Y(x,y) = k_2 Z_y(x,y)$. The subscript on Z denotes partial differentiation. Assume that the errors in the predicted values are stationary (that is, the statistics do not depend on (x,y)), with zero mean. Using $E[.]$ to denote the expected value, or ensemble average, the spatial covariance function for Z, as a function of "lags" s and t, is

$$R(s,t) = E[Z(x,y)Z(x+s,y+t)] = E[Z(x-s,y-t)Z(x,y)] \ .$$

The latter equality follows from stationarity. Under the assumption that the order of partial differentiation and the expected value can be interchanged the cross covariance functions, and the covariance functions for the derived variables are

$$E[Z(x,y)X(x+s,y+t)] = E[Z(x,y)k_1 Z_x(x+s,y+t)] =$$
$$E[Z(x,y)k_1 Z_s(x+s,y+t)] = k_1 E[Z(x,y)Z(x+s,y+t)]_s = k_1 R_s(s,t),$$

$$E[Z(x,y)Y(x+s,y+t)] = E[Z(x,y)k_2 Z_y(x+s,y+t)] =$$
$$E[Z(x,y)k_2 Z_t(x+s,y+t)] = k_2 E[Z(x,y)Z(x+s,y+t)]_t = k_2 R_t(s,t),$$

$$E[X(x,y)Z(x+s,y+t)] = E[X(x-s,y-t)Z(x,y)] =$$
$$E[k_1 Z_x(x-s,y-t)Z(x,y)] = E[-k_1 Z_s(x-s,y-t)Z(x,y)] =$$
$$-k_1 E[Z(x,y)Z(x+s,y+t)]_s = -k_1 R_s(s,t),$$

$$E[X(x,y)X(x+s,y+t)] = E[X(x,y)k_1 Z_x(x+s,y+t)] =$$
$$k_1 E[X(x,y)Z(x+s,y+t)]_s = k_1 E[X(x-s,y-t)Z(x,y)]_s =$$
$$k_1 E[k_1 Z_x(x-s,y-t)Z(x,y)]_s = -k_1^2 E[Z_s(x-s,y-t)Z(x,y)]_s =$$
$$-k_1^2 E[Z(x,y)Z(x+s,y+t)]_{ss} = -k_1^2 R_{ss}(s,t),$$

$$E[X(x,y)Y(x+s,y+t)] = E[X(x,y)k_2 Z_y(x+s,y+t)] =$$
$$E[X(x,y)k_2 Z_t(x+s,y+t)] = k_2 E[X(x,y)Z(x+s,y+t)]_t =$$
$$k_2 E[k_1 Z_x(x-s,y-t)Z(x,y)]_t = k_2 E[-k_1 Z_s(x-s,y-t)Z(x,y)]_t =$$
$$-k_1 k_2 E[Z(x,y)Z(x+s,y+t)] = -k_1 k_2 R_{ts}(s,t)$$

$$E[Y(x,y)Z(x+s,y+t)] = E[k_2 Z_y(x-s,y-t)Z(x,y)] =$$
$$E[-k_2 Z_t(x-s,y-t)Z(x,y)] = -k_2 E[Z(x,y)Z(x+s,y+t)]_t =$$
$$-k_2 R_t(s,t) \ ,$$

$$E[Y(x,y)X(x+s,y+t)] = E[Y(x,y)k_1Z_x(x+s,y+t)] =$$
$$E[Y(x,y)k_1Z_s(x+s,y+s)] = k_1E[Y(x-s,y-t)Z(x,y)]_s =$$
$$k_1E[k_2Z_y(x-s,y-t)Z(x,y)]_s = k_1E[-k_2Z_t(x-s,y-t)Z(x,y)]_s =$$
$$-k_1k_2E[Z(x,y)Z(x+s,y+t)]_{st} = -k_1k_2R_{st}(s,t),$$

$$E[Y(x,y)Y(x+s,y+t)] = E[Y(x,y)k_2Z_y(x+s,y+t)] =$$
$$k_2E[Y(x,y)Z(x+s,y+t)]_t = k_2E[Y(x-s,y-t)Z(x,y)]_t =$$
$$k_2E[k_2Z_y(x-s,y-t)Z(x,y)]_t = -k_2^2E[Z_t(x-s,y-t)Z(x,y)] =$$
$$-k_2^2E[Z(x,y)Z(x+s,y+t)]_{tt} = -k_2^2R_{tt}(s,t) .$$

Note that while the covariance functions are symmetric, the cross covariance functions are antisymmetric, which accounts for the sign change that comes from changing the order of the product in the expected value. This means, among other things, that the cross covariance must be zero at zero lag values. This behavior can be seen in the plots of the various functions in Bergman (1979) and Schlatter, et. al. (1976). In those papers, the signs which appear above also appear, while in Thiébaux (1985) and Pedder and Thiébaux (1986), they are absent. This can be explained from the order in which processes are carried out. In the above, if the observation points are (x_i,y_i), then the lags for a particular pair (with subscripts i and j, say) are $(s,t) = (x_j-x_i,y_j-y_i)$, and the covariance function for Z can be considered as

$$\tilde{R}(x_i,y_i,x_j,y_j) = R(x_j-x_i,y_j-y_i) =$$
$$E[Z(x,y)Z(x+x_j-x_i,y+y_j-y_i) = E[Z(x+x_i,y+y_i)Z(x+x_j,y+y_j)].$$

Now, if we consider the cross covariance, and think of the points (x_i,y_i) and (x_j,y_j) as being variables, rather than fixed points, then

$$E[X(x+x_i,y+y_i)Y(x+x_j,y+y_j)] = [k_1 Z_x(x+x_i,y+y_i)Y(x+x_j,y+y_j)] =$$
$$k_1 E[Z_{xi}(x+x_i,t+y_i)k_2 Z_y(x+x_j,y+y_j)] =$$
$$k_1 k_2 E[Z(x+x_i,y+y_i)Z(x+x_j,y_j)]_{xi\,yj} = \tilde{R}_{xi\,yj}(x_i,y_i,x_j,y_j) .$$

The other covariance and cross covariance functions are handled in a similar manner. Differentiation with respect to x_i then is the negative of differentiation with respect to s, while differentiation with respect to x_j is the same as differentiation with respect to s and therefore the apparent loss of the signs.

3.2 Some Necessary Properties

In order for the covariances of the derived functions and the cross covariance functions to exist, certain conditions must be satisfied by the function R(s,t). These have been alluded to by Buell (1972), and are given by Julian and Thiébaux (1975). The conditions given are for an isotropic covariance function. For the moment, suppose that s represents the lag distance (in the above, $(s^2 + t^2)^{1/2}$), and that the covariance function R(s) is isotropic. Then the conditions cited are

$$\lim_{s>0} \frac{R_s(s)}{s} \text{ is finite, and } \lim_{s>0}\left[\frac{R_s(s)}{s} - R_{ss}(s) \right] = 0 .$$

When one considers that $R_s(0)$ must be zero, the first limit is the definition of the second derivative at s=0, hence existence of the limit means that the covariance function must be twice differentiable at s=0. The second limit then says that the

second derivative is continuous at s=0. Thus the theorem given by Julian and Thiébaux can be replaced with a simpler one:

Theorem 1: If R(s) is an isotropic covariance function for Z in two dimensions, then the covariance functions for the partial derivatives of Z exist at s=0 if and only if R(s) is twice continuously differentiable at s=0.

3.3 Anisotropic Functions

It has been contended that isotropic covariance functions do not adequately model the forecast error statistics and that gains can be made by using anisotropic functions. See Thiébaux (1976, 1977, 1985), and Thiébaux, et. al. (1985) for development and discussion of product forms of covariance functions. Use of products of single dimensional functions has the advantage of carrying over desirable properties to higher dimensions, as well as being able to use essentially one dimensional structures and techniques. On the other hand, perusal of contour plots of product functions show that zero crossings of the functions occur along grid lines, and it is easy to see this will always happen. This may be undesirable behavior, and almost certainly it is not the kind of behavior seen in the error statistics.

Another form of anisotropy is possible, one which results from scaling differently in two orthogonal directions, then using an isotropic function in the scaled variables. Presumably, but not necessarily, the two directions would be the longitude and latitude directions. This would result in the zero crossings in

the contour plots of the function being ellipses with axes in the two directions; all contours would have the same shape. The eccentricity of the ellipse is a measure of the anisotropy of the error statistics. It would be easy to allow rotation along with the scaling to obtain ellipses of constant "distance" with any axis orientation. No references to use of this kind of anisotropy in the meteorological literature have come to my attention. The properties of any such functions are those of isotropic functions, of course, since the anisotropy arises purely from a rotation and scaling.

3.4 Isotropic Functions

The use of isotropic functions in two or more dimensions which have been derived from one dimensional considerations can possibly lead to nonpositive definite functions. For example, Ripley (1981, p. 11) quotes a result of Matérn (1960), which gives a lower bound for isotropic positive definite functions in several dimensions. The result means that positive definite functions in two dimensions are necessarily bounded below by -0.403 (the minimum value of $J_0(s)$), while in three dimensions the bound is -0.218 . Thus any oscillatory positive definite function in one dimension which takes on values less than -0.403 cannot be an isotropic positive definite function in two dimensions. A positive definite function which has parameters to separately control the oscillation frequency and the decay can probably be made into a nonpositive definite isotropic function in two dimensions. In particular, a function such as

$$f(s) = \cos(as)\exp(-bs)$$

can be made nonpositive definite by suitable choice of parameters, say a = 5 and b = .1 . This result also applies to the isotropic version of the second order auto-regressive (SOAR) function as well, although a restriction on the ratio of the parameters in the function will guarantee it is positive definite in two dimensions. In practice it has been shown that one of the parameters tends to be zero in the SOAR when fit to meteorological data (Thiébaux, et. al. (1985), and Section 4 of this report). This satisfies the necessary requirement, and hence the function as used is positive definite. The details will be given later.

There is a one-to-one correspondence between covariance functions in one dimension and isotropic covariance functions in two dimensions. Matheron (1973) gives a way of generating an isotropic d-dimensional covariance function from a one dimensional covariance function, the so-called "turning band" method. The relation is

$$C_d(s) = K\int_0^1 C_1(vs)(1-v^2)^{(d-3)/2}\,dv\ ,$$

where K is a constant that is unimportant for our purposes. In two dimensions, this gives

$$C_2(s) = K\int_0^1 C_1(vs)(1-v^2)^{-1/2}\,dv\ .$$

Although Matheron doesn't give the result, it is possible to invert this relation to show the one-to-one relationship. A

sketch of the inversion process follows. A change of variables in the previous expression gives

$$C_2(s) = K\int_0^s C_1(t)(s^2-t^2)^{-1/2}\,dt\ .$$

A further change of variables, $s^2 = x$, and $t^2 = y$, yields

$$C_2(x^{1/2}) = K\int_0^x [C_1(y^{1/2})(2y)^{-1/2}](y-x)^{-1/2}\,dt\ .$$

This is Abel's equation for $K\,C_1(y^{1/2})(2y)^{-1/2}$, and the solution is well known (see Hochstadt, 1972) and is given by

$$C_1(x^{1/2}) = K'x^{1/2}\,\frac{d}{dx}\int_0^x C_2(y^{1/2})(x-y)^{-1/2}\,dy\ ,$$

where K' is a different constant, and upon substitution for s and t once again, gives

$$C_1(s) = K's\,\frac{d}{d(s^2)}\int_0^s C_2(t)(s^2-t^2)^{-1/2}2t\,dt\ .$$

The correspondence between covariances in one dimension and three dimensions is easier to invert, and is given by Ripley (1981). There the relation is

$$C_3(s) = \int_0^1 C_1(vs)\,dv, \text{ and } C_1(s) = \frac{d}{ds}\,[sC_3(s)]\ .$$

While this characterization of multidimensional isotropic covariance functions is interesting, and can in fact be used to generate isotropic multidimensional covariance functions, it does not easily answer the question as to whether or not a particular one dimensional function is an isotropic positive definite function in more dimensions. One way to answer such a question is to

use the characterization of positive definite functions as Fourier transforms of probability density functions (or alternatively, as functions whose Fourier transform is positive). The Fourier transform of an isotropic function C(s) in two dimensions becomes (essentially) the Hankel transform of $s^{1/2}C(s)$. It may be considerably easier to look at the one dimensional Fourier transform, however, so it would be useful to have a sufficient condition on the Fourier transform of the function which would guarantee it is an isotropic positive definite function in two dimensions. Such a condition will now be derived.

Let $C_1(s)$ be a positive definite function of one variable. By the characterization in the previous section, write

$$(1) \quad C_1(s) = \int_0^\infty \cos(rs)\, h(r)\, dr,$$

for some probability density function h(r) (i.e., $h(r) \geq 0$, with integral equal 1). Then, under what conditions will $C_1(s)$ be the two dimensional Fourier transform of an isotropic probability density function? Such a transform is necessarily isotropic. A function g(s) is sought so that

$$(2) \quad C_1(r) = \int_0^\infty J_0(rs)\, s\, g(s)\, ds \quad .$$

This expression is inverted using the Hankel transform, giving

$$(3) \quad g(s) = \int_0^\infty J_0(sr)\, r\, C_1(r)\, dr.$$

Then, using (1) in (3), and interchanging the order of integration, followed by integration by parts yields

$$g(s) = \int_0^\infty J_0(sr)\, r \left(\int_0^\infty \cos(tr)\, h(t)\, dt \right) dr =$$

$$\int_0^\infty h(t) \left(\int_0^\infty J_0(sr)\, r \cos(tr)\, dr \right) dt =$$

$$\int_0^\infty h(t) \left(-\frac{d}{dt} \int_0^\infty J_0(sr) \sin(tr)\, dr \right) dt =$$

$$\int_0^\infty h'(t) \left(\int_0^\infty J_0(sr) \sin(tr)\, dr \right) dt \quad ,$$

and then,

$$(4) \qquad g(s) = -\int_s^\infty h'(t)/(t^2-s^2)^{1/2}\, dt \ .$$

The last equality uses the Hankel transform of $r^{-1/2}\sin(tr)$.

In order for g(s) to be a probability density function it must be nonnegative with integral equal to one. It is easy to show (again, interchanging the order of integration) that the integral is equal to one. Necessary and sufficient conditions for the nonnegativity of g(s) are harder. The following is apparent.

Theorem 2: A sufficient condition for $C_1(s)$ to be a valid isotropic covariance function in two dimensions is that h(t) be a monotone decreasing ($h'(t) \leq 0$) function.

This condition seems unnecessarily restrictive, and further is not as revealing as would be convenient since the condition is on the Fourier cosine transform of $C_1(s)$ rather than $C_1(s)$ itself. Nonetheless, the condition can be used to show the following results, which are of definite interest.

(1) Consider the exponentially damped cosine function,

$$C(s) = \cos(as)e^{-bs}.$$

The Fourier cosine transform of this function is

$$h(t) = F(C)(t) = \frac{b(b^2+a^2+t^2)}{[b^2+(a-t)^2][b^2+(a+t)^2]} .$$

Inspection of $h'(t)$ shows that if $b^2 \geq 3a^2$, it is nonpositive for all t, and hence $h(t)$ is monotone decreasing under that constraint.

(2) Consider the second order autoregressive (SOAR) covariance function,

$$C(s) = [\cos(as) + (b/a)\sin(as)]e^{-bs}.$$

The Fourier cosine transform of this function is

$$h(t) = F(C)(t) = \frac{2b(b^2+a^2)}{[b^2+(t-a)^2][b^2+(t+a)^2]} .$$

Inspection of $h'(t)$ reveals that if $b^2 \geq a^2$, it is nonpositive for all t, and thus $h(t)$ is monotone decreasing under that constraint. The final result is that each of the above $C(s)$ is an isotropic positive definite function, hence is a covariance function if the appropriate inequality on the parameters is satisfied.

(3) Consider the special case of the damped cosine function

$$C(s) = [A + (1-A)\cos(as)](1 + (bs)^2)^{-1/2} .$$

The Fourier transform of this function is

$$h(t) = F(C)(t) =$$

$$(2b)^{-1}\{(1-A)[K_0(|t-a|/b) + K_0(|t+a|/b)] + AK_0(t/b)\} .$$

Because the modified Bessel function K_0 becomes unbounded as the argument tends to zero, for $A \neq 1$, the Fourier transform must be

increasing as t approaches a through values smaller than a. For t greater than a, and possibly for some values smaller than a, the function is decreasing. Thus the sufficient conditions given above are not met, and it is easy to find configurations of (x,y) points and parameter values A, a, and b for which the resulting "covariance" matrix is not positive definite. The two dimensional Fourier transform of C(s) (the Hankel transform of $s^{1/2}C(s)$) has so far eluded the author, so it is presently unknown if there are parameter values (other than for A = 1) which will yield a positive definite function.

(4) Consider the Bessel function $J_0(as)$. The Fourier transform of this function is

$$h(t) = F(C)(t) = \begin{cases} 0 & , \ t<a \\ t^{1/2}/(t^2-a^2)^{1/2} & , \ t>a \ . \end{cases}$$

This function is easily seen to be monotone decreasing for t>a, and thus the Bessel function $J_0(as)$ is an isotropic covariance function in two dimensions. Note however, that to apply the above results there are some technical details that must be considered because of the infinite jump discontinuity at t=a.

The above results concerning several functions proposed for use as isotropic covariance functions in two dimensions is useful. The lack of results and empirical evidence against the damped cosine being positive definite negate the results noted in the next section where we see that the fitting power of the function is very good. These aspects of the function will be discussed further in the next section.

3.5 Summary

The contents of this section contain some useful information for the construction of positive definite functions and testing of functions for positive definiteness. When possible, the two dimensional Fourier transform of $C_1(s)$ can be used to decide whether or not the function is positive definite. When the two dimensional Fourier transform cannot be obtained in closed form, Theorem 2 can give some information if the one dimensional Fourier transform is available in closed form. While the condition given by Theorem 2 is only sufficient, and not necessary, it has been shown to be useful in investigating some functions which have been proposed for use as isotropic covariance functions in two dimensions.

4.0 Some Experiments with Isotropic Covariance Functions

4.1 Introduction

The work reported in this section was conceived to help determine something about the overall fitting properties of various suggested covariance functions. The term "overall fitting properties" is meant to include not only the ability of the function to model a reasonably complicated true covariance function, but also its performance when used in a statistical interpolation scheme with several different observation patterns.

The approach for this project was to begin with published actual data, and then construct a "true", or model, covariance function, by a least squares fit to the data from a certain class of covariance functions. Functions from other classes would be fit to the same data, again in the least squares sense, and these "assumed" covariance functions would then have their analysis performance measured against that of the optimum model. I believe the results to be discussed give some insight into what classes of functions have adequate fitting ability for modeling actual forecast error statistics, and also show how much skill is lost (in the idealized case) by use of inaccurate covariance functions.

The results given here consist of plots of assumed correlation functions together with the model (true) correlation function, plots of the contours of expected errors, and tables showing expected root-mean-square (erms) errors (relative to the standard deviation of the first-guess error) over three grids of

points and associated observation locations. The expected errors were computed as in Seaman (1983). The results obtained with various assumed correlation functions in the SI scheme are discussed in detail.

4.2 The Model Correlation Function

The data for the covariance function was obtained (by hand) from Lonnberg (1982). The data taken was plotted points from a covariance function of the type used by ECMWF, in this case a five term (i.e., n=5) Bessel series of the form

$$(1) \quad \sum_{i=1}^{n} A_i J_0(s*k_i/R) + A_0 \ ,$$

where k_i is the i^{th} zero of the Bessel function $J_0(s)$, and R is the radius of the region of interest. This function is positive definite as an isotropic function in two dimensions provided the coefficients A_i are all positive. In Lonnberg, R was 2000 km. In this work, distance was measured in degrees, and the radius was scaled to 30°.

Least squares fits to the data by functions of the type (1) for four, five, and six terms were computed. While the original paper indicated a series with five terms generated the data, it was found that six terms yielded all positive coefficients and a significant reduction in the residual over five terms. Thus, it was decided to adopt the six term series as the model covariance function. This six term series would also be marginally harder to approximate using other classes of covariance functions. The data and the fits using four and six terms are shown in Figure 1,

and the coefficients are given in Table 1, along with other data. The intercept values of the approximations were 0.8270 and 0.8592 for four and six terms, respectively. This occurs because the data represents the spatial correlation of the first-guess plus observation error, thus the intercept is a function of the ratio of the standard deviations of first-guess and observation error. The effects of this kind of discrepancy will be discussed in section 4.4. The correlation function for first-guess error is the approximation normalized to have value one at s=0, of course.

4.3 The Grid and Observation Point Sets

Three grids and associated point sets were selected for studying the expected errors of statistical interpolation schemes based on various assumed covariance functions. All were based on the approximate locations of radiosonde data (from Wahba and Wendelberger (1980) and Ghil, et.al. (1981)) within the selected grid. Each grid covered a region which was 30° in longitude and 20° in latitude, and the three were chosen to represent a dense observation set, a partially dense observation set, and a sparse observation set. The regions correspond to the central United States with 36 observations, the eastern United States and western Atlantic Ocean with 25 observations, and the middle Atlantic Ocean with 3 observations. For reference purposes, the three regions will be referred to as the MUS (Mid-US), EC (East Coast), and MA (Mid-Atlantic) regions. The regions and the observation locations can be seen in Figures 2-11, parts (b), (c), and (d), respectively. The regions were gridded at 2.5° intervals for

purposes of computing expected errors, although the erms errors given in Table 1 are only over the interior grid points to minimize edge effects. For contouring purposes the fields were interpolated to finer grids using bicubic spline interpolation.

4.4 The Assumed Correlation Functions and Results

The families of assumed correlation functions fell into 5 classes: (i) Bessel function, (ii) negative squared exponential (sometimes called Gaussian), (iii) autoregressive of order two, (iv) autoregressive of order three, and (v) damped cosine. They will be discussed, along with the results, in turn. Plots of the assumed correlation functions, along with the model correlation function, are shown in part (a) of Figs. 2-11. For fitting purposes, each included a multiplicative parameter which determined the s=0 intercept, and was subsequently dropped to obtain the correlation function. The value of this parameter is of interest, however, because dropping it shifts the curve (upward) to pass through the point (0,1), and thus different fits may be shifted by different amounts, which ultimately affects the fit to the first-guess error correlation function.

Recall that the erms errors given in Table 1 are given as a fraction of standard deviation of the first-guess error. It was assumed that the ratio of the standard deviation of the observation errors to the standard deviation of the first-guess errors was 1/3.

(i) Bessel Function

The reference expected errors were computed using the actual correlation function model, given by Eq. (1) with coefficients as given in Table 1. The results are given in Table 1, and are the smallest expected errors that can be obtained using a correction to first-guess scheme, that is, they are truly optimum. The correlation function is shown in part (a) of Fig. 2, while the contour plots of the expected error for each of the three grid/observation sets is shown in parts (b), (c), and (d).

The results using a four term Bessel function are shown in Fig. 3. Because the intercept of the fit to the data is 0.8270 versus 0.8592, normalization to value one produces a curve which is then predominately above that for the model correlation function, especially for small distances. The result of the poor approximation for small distances is most pronounced over MUS, as seen in Fig. 3a. The effect was small over the sparse part of EC and over MA.

(ii) Negative Squared Exponential (NSE)

The NSE has been recognized as inadequate for modeling error covariances for some time, and the results obtained here confirm that. The assumed form of the function was

$$(2) \quad A + (1-A)e^{-(s/b)^2} \quad .$$

This function is positive definite as an isotropic function in two dimensions for $0 \leq A \leq 1$.

The initial fit was not obtained by least squares, but simply by attempting to fit the model correlation reasonably well for small distances, taking A=0. As shown by Fig. 4a, the fit is reasonably good up to about 6^{o}, and quite poor at greater distances. The expected errors are similar in magnitude to the expected errors for the four term Bessel function, except over MA, where the errors are larger. However, since the errors over MA tend to be large anyway, the relative effect is not as great as one might expect.

The second attempt was by least squares for the parameters A and b. Because the NSE is too flat near the origin, this process yielded an intercept value of 0.8060, shifting the correlation function shown in Fig. 5a so that it is entirely above above the model correlation curve. This results in even poorer performance over MUS and EC than the previous model, due to the inaccurate representation for small distances. The performance over MA was better than the above. The contour plots of expected error are shown in Fig. 5.

Due to the poor performance (compared to the above) obtained by adding a constant to the basic NSE it was decided to attempt to find a better fit by trial and error. No claim is made about any optimality for this function. The results are shown in Fig. 6, and these plots along with the results in Table 1 demonstrate that it is probably not possible to obtain good results overall with a function from the NSE family, and certainly not for the present model correlation function.

(iii) Autoregressive, Order Two (SOAR)

The SOAR model has been suggested as appropriate by Thiébaux (1985) and this is supported by simulations due to Balgovind, et.al. (1983). The model is also the current favorite for incorporation into the U. S. Navy models. The formula given here includes a constant term which is not part of the SOAR model, but which has been noted to improve performance considerably (Thiébaux, et.al., 1985), and those results are confirmed here. The SOAR function with additive constant is

$$(3) \quad A + (1-A)[\cos(as) + (b/a)\sin(as)]e^{-bs} \quad .$$

This function is positive definite (in two dimensions) whenever $a \leq b$, and $0 \leq A \leq 1$. In all cases investigated here, and as has been reported elsewhere, (e.g., Thiébaux, et.al., 1985), the parameter a tends to be essentially zero. In this case the function reduces to

$$(3a) \quad A + (1-A)[1 + bs]e^{-bs} \quad .$$

The initial attempt was a least squares fit to the data with A=0. The intercept obtained was 0.7977, with the resulting correlation curve then being considerably above the model correlation curve between 0^{o} and 15^{o}, as is shown in Fig. 7a. The performance was only slightly better than with any of the previous correlation functions. It was then decided to attempt a least squares fit with the intercept constrained to be 0.8592, the same as obtained for the model correlation function, but again with A=0. The results of this calculation and the

resulting expected error contours are shown in Fig 8. Table 1 shows marginal improvement for all three grid/observation patterns. A third attempt included A in the least squares fit, with no constraint. This resulted in a much closer match to the model correlation function, although the intercept of 0.8441 moved the assumed correlation curve above the model curve for much of the interval. The results are shown in Fig. 9, and Table 1 shows considerable improvement over all previous results, the most improvement being for MUS, and the least for MA.

(iv) Autoregressive, Third Order (TOAR)

The use of the TOAR model has been investigated by Thiébaux, et.al. (1985), including an additive constant. The formula is

$$(4) \quad A + (1-A)[(\bar{a}\cos(as) + \bar{b}\sin(as))e^{-bs} + \bar{c}e^{-cs}] \quad ,$$

where the coefficients $\bar{a}$, $\bar{b}$, and $\bar{c}$ are functions of a, b, and c (see Appendix 1 for the formulas). It is unknown what restrictions (beyond $0 \leq A \leq 1$) on the parameters are required to ensure the function is positive definite as an isotropic function in two dimensions.

The data was fit by least squares with the TOAR function (4). The intercept was 0.8651, which resulted in the curve being slightly below the model correlation curve over most of the range, although the fit was quite close, better than any of the previously discussed functions. The results are given in Fig. 10 and Table 1 and show very close agreement with the optimum possible for all three of the grid/observation sets.

(v) Damped Cosine

The damped cosine function has been suggested by Thiébaux (1976) and Seaman and Hutchinson (1985). The formula is

$$(5) \quad [A + (1-A)\cos(as)]/[1 + (bs)^2]^c \ .$$

It is unknown whether the function is positive definite as an isotropic function in two dimensions, but the evidence in Section 3.4 (for c=.5), while inconclusive, seems to indicate it is not. In practice, of course, the function may be positive definite when the observation points are restricted to certain regions.

The data was fit with the function (5), under the restriction c=.5. The intercept was 0.8565, which resulted in a very slight raising of the curve relative to the model correlation function. The resulting fit is excellent for small distances and very good over the entire range, as is seen in Fig. 11a. Table 1 shows that the best results for any of the assumed correlation functions are achieved here.

(vi) Variations

The expected error computations for a number of variations of the above functions were also performed. The principal variation was to fit the data only over the first half of the interval, $(0^o, 15^o)$. The effect of this was to generally (though not always) increase the erms errors over MUS and EC, while not affecting the results over MA. In the damped cosine, the exponent c was chosen by least squares, along with the other

parameters, and resulted in a slightly better fit to the correlation function, especially at larger distances. However, the coefficient A was slightly greater than 1. Whatever the positive definiteness properties of the function, having A>1 will certainly make it non-positive definite. Although the graphical results are not shown, the coefficients and erms errors are given in Table 1 for the additional assumed correlation functions.

4.5 Conclusions

The principal conclusion to be drawn is that the correlation family used in practical analysis should embody a sufficient number of parameters to fit the forecast error statistics reasonably well. Further, it is most important that the data be fit accurately for small distances. In order to ensure a better fit for small distances, it may be worthwhile to enforce the intercept of the correlation for the first-guess plus observation errors <u>if</u> the ratio of standard deviations of the two errors is known <u>accurately</u>. The effect of scaling to obtain the correlation function, and the apparent shift up or down can possibly be compensated for by artificially varying the ratio of first-guess to observation errors, as well, although it seems more desirable to enforce this ratio in the correlation function fitting process.

As noted above, clearly the most important region for the fit to the correlation function to be accurate is for small distances. Over the sparsely observed region, MA, and to a lesser extent over the EC region, the overall erms errors were only slightly affected by the assumed correlation function. In

the case of the MA region it is noted that the error contours are relatively unaffected except near the observations. Since the errors in the remote part of the region dominate the overall error, the choice of assumed correlation function has relatively small influence. On the other hand, over the densely observed region, an accurate fit at small distances was most important. The NSE correlation function, while not performing well, illustrates the above nicely, as shown in Figs 4 and 6. Even though the fit shown in Fig. 4a is poor for distances of more than 6°, compared to the fit in Fig. 6a, the erms errors over MUS and EC are smaller due to the more accurate fit for small distances by the former function. Of course the erms errors over MA are poorer due to the very bad fit at large distances in Fig. 4a.

There appear to be several good candidates for use as two dimensional isotropic correlation functions, including SOAR, TOAR, and damped cosine, given by Eqs. (3), (4), and (5), respectively. While the fitting power for the latter two are greater (there are a greater number of parameters for those two), the choice of SOAR seems reasonable and adequate for a number of reasons: (1) The SOAR (with the additive constant) embodies a sufficient number of parameters to allow oscillation and decay with distance. (2) The SOAR has some credibility as the spatial correlation function of an innovation process, but in one dimension rather than two, and further the only evidence that it might be near the right one is that cited previously in Balgovind, et.al. (1983). (3) The SOAR was demonstrated here to be positive definite as an isotropic function in two dimensions, under

what seems in the practical case to be a mild restriction on the parameters. (4) While the TOAR is also the spatial correlation function (again in one dimension) for an innovation process, based on this limited study it does not appear to be significantly better than SOAR. (4) The positive definiteness properties of the TOAR are not known, although it seems reasonable to speculate that it is positive definite as an isotropic function in two dimensions under some restrictions on the parameters. (5) While the fitting ability of the damped cosine seems to be at least as good as the TOAR, and while it is positive definite in one dimension, evidence indicates it may not be positive definite as an isotropic function in two dimensions, regardless of parameter restrictions. The availability of other acceptable alternatives seems to make it prudent to preclude the use of the damped cosine in practical situations.

Finally, it is pointed out that all of the functions except the four term Bessel function and the NSE perform very well. Table 1 shows, for example, that the SOAR is only a little more than 1% of the standard deviation of the first-guess error poorer than optimal over MUS and EC, and less than .1% poorer over MA.

5. Acknowledgements

I acknowledge some very useful discussions on a continuing basis with Drs. Ed Barker and Jim Goerss at the Naval Environmental Prediction Research Facility. Their criticism and advice have contributed greatly to shaping this work and its final form in this report. In addition, Dr. Barker performed many of the least squares fits for the covariance functions at NEPRF using the ACM algorithm #573 (Dennis, et.al., 1981). Thanks also go to Dr. Gordon E. Latta for his help in dealing with transforms and integrals in general. Finally, most of the computing was performed on the IBM 3033AP at the Naval Postgraduate School.

References

Alaka, M. A., and E. C. Elvander, 1972: Optimum interpolation from observations of mixed quality. Mon. Wea. Rev., **100**, 612-624.

Balgovind, R., A. Dalcher, M. Ghil, and E. Kalnay, 1983: A stochastic-dynamic model for the spectral structure of forecast error statistics. Mon. Wea. Rev., **111**, 701-722.

Bergman, K. H., 1979: Multivariate analysis of temperatures and winds using optimum interpolation. Mon. Wea. Rev., **107**, 1423-1444.

Bochner, S., 1959: **Lectures on Fourier Integrals** (translated from the original by M. Tenenbaum and H. Pollard). Princeton University Press, Princeton, NJ.

Buell, C. E., 1972: Correlation functions for wind and geopotential on isobaric surfaces. J. Appl. Met., **11**, 51-59.

Creutin, J. D., and C. Obled, 1982: Objective analyses and mapping techniques for rainfall fields: An objective comparison. Water Resources Research, **18**, 413-431.

Dennis, J. E. Jr., D. M. Gay, and R. E. Welsch (1981): An adaptive nonlinear least squares algorithm. ACM TOMS **7**, 348-368 and Algorithm 573: NL2SOL, pp. 369-383.

Franke, R. 1985: Sources of error in objective analysis. Mon. Wea. Rev., **113**, 260-270.

Gandin, L. S., 1963: Objective Analysis of Meteorological Fields. Translated from Russian by Israel Program for Scientific Translations, 1965, 242 pp. [NTIS **TT65-50007**].

Ghil, M., S. Cohn, J. Tavantzis, K. Bube, and E. Isaacson, 1981: Applications of estimation theory to numerical weather prediction. In Bengtsson, L., M. Ghil, and E. Kallen, editors, **Dynamic Meteorology: Data Assimilation Methods**, Springer-Verlag, New York, pp.139-224.

Hochstadt, H., 1973: **Integral Equations**. John Wiley & Sons, New York.

Julian, P. R., and H. J. Thiébaux, 1975: On some properties of correlation functions used in optimum interpolation schemes. Mon. Wea. Rev., **103**, 605-616.

Lonnberg, P., 1982: Structure functions and their implications for higher resolution analysis. In, **Proceedings, Workshop on Current Problems in Data Assimilation**, ECMWF, November 8-10, 1982, pp. 142-178.

Lorenc, A. C., 1981: A global three dimensional multivariate statistical interpolation scheme. Mon. Wea. Rev., **109**, 701-721.

Matérn, B., 1960: **Spatial Variation**, Meddelanden fran Statens Skogsforskningsinstitut **49**,5, pp. 1-144.

Matheron, G., 1973: The intrinsic random functions and their applications. Adv. in Appl. Prob., 5, 439-468.

McPherson, R. D., 1982: Optimum interpolation: Practical aspects of operational application. In, Williamson, D., editor, **The Interaction Between Objective Analysis and Initialization**, NCAR Technical Note NCAR/TN-204+PROC, pp 7-12.

Priestly, M. B., 1981: **Spectral Analysis and Time Series, Vol. 1: Univariate Series; Vol. 2: Multivariate Series, Prediction and Control**. Academic Press, New York.

Ripley, B. D., 1981: **Spatial Statistics**. John Wiley & Sons, New York.

Rutherford, I. D., 1972: Data assimilation by statistical interpolation of forecast error fields. J. Atmos. Sci., **29**, 809-815.

Schlatter, T. W., 1975: Some experiments with a multivariate statistical objective analysis scheme. Mon. Wea. Rev., **103**, 246-257.

Schlatter, T. W., G. W. Branstator, and L. G. Thiel, 1976: Testing a global multivariate statistical objective analysis scheme with observed data. Mon. Wea. Rev., **104**, 765-783.

Seaman, R. S., 1983: Objective analysis accuracies of statistical interpolation and successive correction schemes. Aust. Meteor. Mag., **31**, 225-240.

Seaman, R. S., and M. F. Hutchinson, 1985: Comparative real data tests of some objective analysis methods by withholding observations. Aust. Met. Mag., **33**, 37-46.

Steinitz, G., et.al., 1971: Optimum station network in the tropics. J. Appl. Meteor. **10**, 364-369.

Stewart, J., 1976: Positive definite functions and generalizations, an historical survey. Rocky Mt. J. of Math., **6**, 409-434.

Thiébaux, H. J., 1975: Experiments with correlation representations for objective analysis. Mon. Wea. Rev., **103**, 617-627.

Thiébaux, H. J., 1976: Anisotropic correlation functions for objective analysis. Mon. Wea. Rev., **104**, 994-1002.

Thiébaux, H. J., 1977: Extending estimation accuracy with anisotropic interpolation. Mon. Wea. Rev., **105**, 691-699.

Thiébaux, FH. J. 1981: The kinetic energy spectrum vis-a'-vis a statistical model for geopotential. Tellus, **33**, 417-427.

Thiébaux, H. J. 1985: On approximations to geopotential and wind-field correlation structures. Tellus, **37A**, 126-131.

Thiébaux, H. J., H. L. Mitchell, and D. W. Shantz, 1985: Horizontal structure of hemispheric forecast error correlations. **Preprints, Seventh Conference on Numerical Weather Prediction**, 17-26.

Thiébaux, H. J., and M. A. Pedder, 1985: **Spatial Objective Analysis**. Preprint.

Yudin, M. I., 1961: Some regularities in the structure of the geopotential field. Trudy GGO, **121**, 3-18.

Parameter Values and erms Errors
Model Correlation is Six Term Bessel

Assumed Correlation Function	Parameters a,b,c	A, A_i	erms MUS	erms EC	erms MA
6 T Bessel		0.2474	0.2667	0.3752	0.7483
		0.3335			
		0.1844			
		0.1031			
		0.0362			
		0.0554			
		0.0400			
4 T Bessel		0.2811	0.3046	0.4088	0.7503
		0.3090			
		0.2213			
		0.0930			
		0.0956			
NSE	10.0	0.0	0.3047	0.4184	0.7822
NSE	14.88	0.3200	0.3688	0.5282	0.7631
NSE	10.0	0.2500	0.3098	0.4158	0.7541
SOAR	0.0	0.0	0.3034	0.4022	0.7562
		0.1215			
SOAR	0.0	0.0	0.2931	0.3968	0.7562
	0.1374				
SOAR	0.0	0.2722	0.2780	0.3859	0.7491
	0.2055				
TOAR	0.4732	0.1974	0.2717	0.3794	0.7485
	0.3828				
	0.0914				
Dmpd Cos	0.4749	0.9592	0.2686	0.3779	0.7486
	0.1367				
	0.5000				
NSE*	15.0	0.0	0.3619	0.4414	0.7649
NSE*	12.31	0.3205	0.3474	0.4299	0.7593
SOAR*	0.0	0.3758	0.2743	0.3825	0.7495
	0.2654				
TOAR*	0.4468	-5.9965	0.2697	0.3801	0.7514
	0.1482				
	0.0052				
Dmpd Cos*	1.2236	1.0027	0.2749	0.3734	0.7491
	0.1507				
	0.5000				
Dmpd Cos	0.7009	1.0105	0.2692	0.3779	0.7484
	0.2069				
	0.3753				
Dmpd Cos*	0.7987	1.0147	0.2706	0.3784	0.7485
	0.2350				
	0.3317				

Table 1

* These correlation functions were obtained by least squares fit over the interval $(0^{\circ}, 15^{\circ})$

Figure Captions

Figure 1: The data points and least squares fits by four and six term Bessel functions.

Figure 2: (a) Six term Bessel correlation function (true and assumed). (b) Expected root-mean-square error contours for the MUS grid and observation point set for the correlation functions shown in (a). (c) As in (b) for the EC grid and observation point set. (d) As in (b) for the MA grid and observation point set.

Figure 3: (a) Six term Bessel correlation function (true) and four term Bessel correlation function (assumed). (b), (c), and (d) As in corresponding parts of Fig. 2 for the correlation functions shown in (a).

Figure 4: (a) Six term Bessel correlation function (true) and negative squared exponential correlation function obtained by visual fit for small distances (assumed). (b), (c), and (d) As in corresponding parts of Fig. 2 for the correlation functions shown in (a).

Figure 5: (a) Six term Bessel correlation function (true) and negative squared exponential plus constant correlation function obtained by least squares fit (assumed). (b), (c), and (d) As in corresponding parts of Fig. 2 for the correlation functions shown in (a).

Figure 6: (a) Six term Bessel correlation function (true) and negative squared exponential plus constant correlation function obtained by visual fit (assumed). (b), (c), and (d) As in corresponding parts of Fig. 2 for the correlation functions shown in (a).

Figure 7: (a) Six term Bessel correlation function (true) and second order autoregressive correlation function obtained by least squares (assumed). (b), (c), and (d) As in corresponding parts of Fig. 2 for the correlation functions shown in (a).

Figure 8: (a) Six term Bessel correlation function (true) and second order autoregressive correlation function obtained by least squares with intercept constaint (assumed). (b), (c), and (d) As in corresponding parts of Fig. 2 for the correlation functions shown in (a).

Figure 9: (a) Six term Bessel correlation function (true) and second order autoregressive plus constant correlation function (assumed). (b), (c), and (d) As in corresponding parts of Fig. 2 for the correlation functions shown in (a).

Figure 10: (a) Six term Bessel correlation function (true) and third order autoregressive plus constant correlation function (assumed). (b), (c), and (d) As in corresponding parts of Fig. 2 for the correlation functions shown in (a).

Figure 11: (a) Six term Bessel correlation function (true) and damped cosine with exponent 1/2 correlation function (assumed). (b), (c), and (d) As in corresponding parts of Fig. 2 for the correlation functions shown in (a).

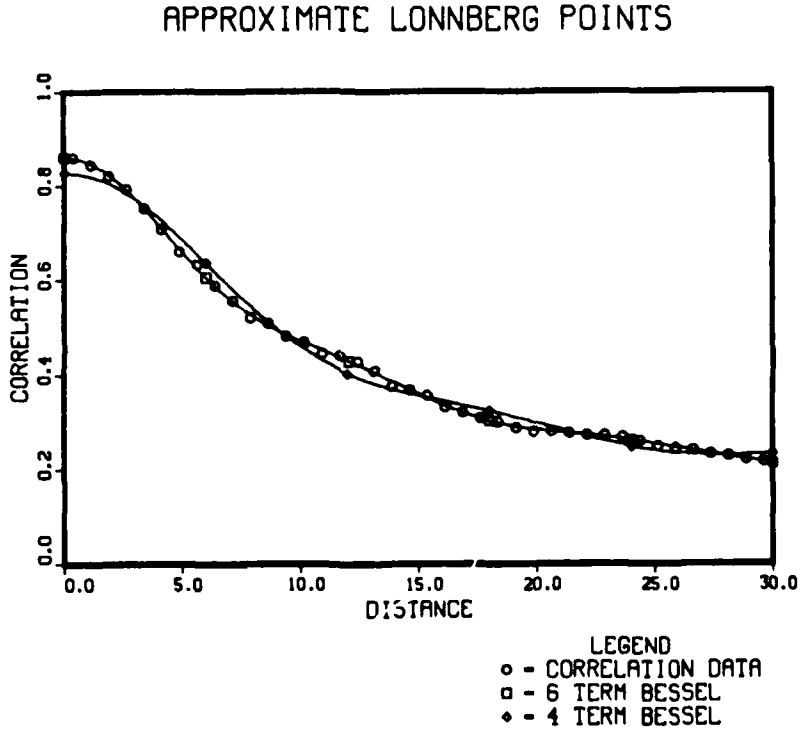
APPROXIMATE LONNBERG POINTS
CORRELATION
1.0
0.8
0.6
0.4
0.2
0.0
0.0
5.0
10.0
15.0
20.0
25.0
30.0
DISTANCE
LEGEND
o - CORRELATION DATA
□ - 6 TERM BESSEL
◇ - 4 TERM BESSEL

FIGURE 1

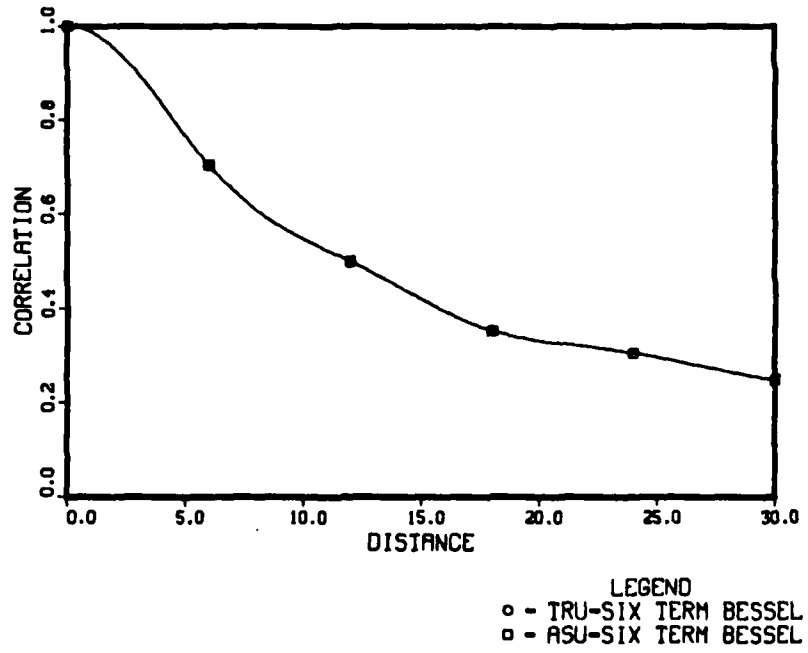
CORRELATION FUNCTIONS
CORRELATION
0.0
0.2
0.4
0.6
0.8
1.0
0.0
5.0
10.0
15.0
20.0
25.0
30.0
DISTANCE
LEGEND
o - TRU-SIX TERM BESSEL
□ - ASU-SIX TERM BESSEL

(a)

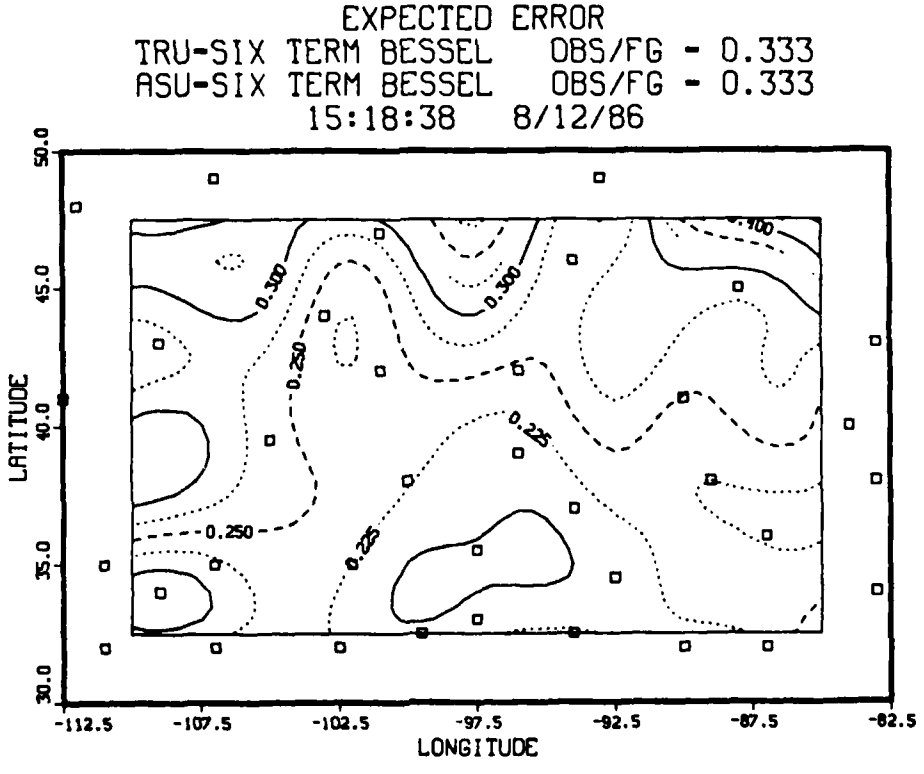
EXPECTED ERROR
TRU-SIX TERM BESSEL OBS/FG - 0.333
ASU-SIX TERM BESSEL OBS/FG - 0.333
15:18:38 8/12/86
LATITUDE
50.0
45.0
40.0
35.0
30.0
-112.5
-107.5
-102.5
-97.5
-92.5
-87.5
-82.5
LONGITUDE
0.300
0.250
0.225

(b)

FIGURE 2

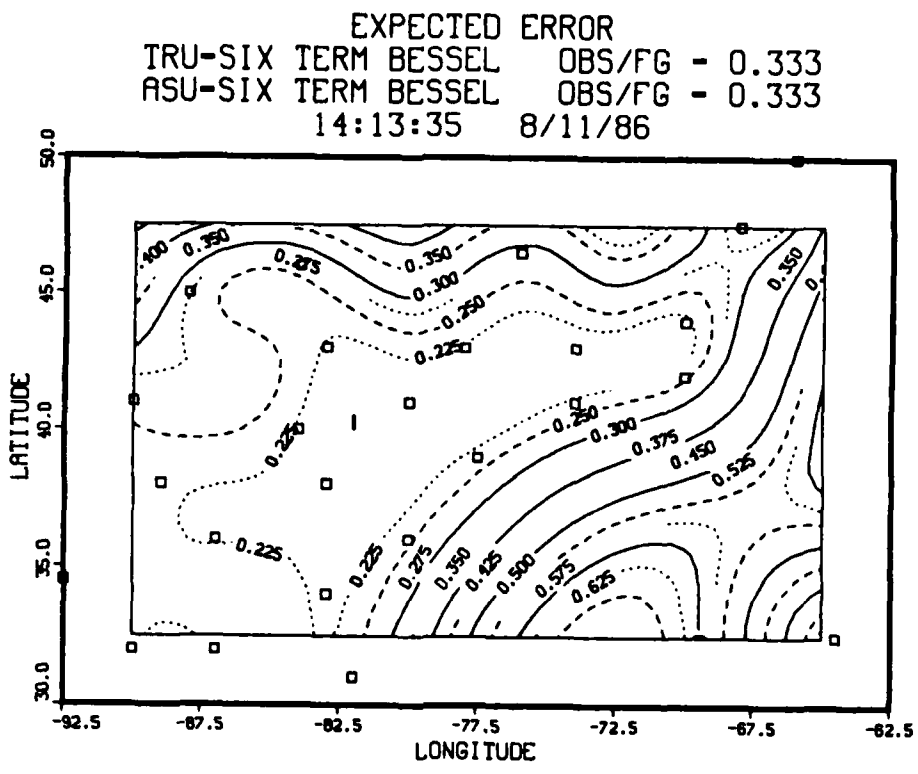
EXPECTED ERROR
TRU-SIX TERM BESSEL OBS/FG - 0.333
ASU-SIX TERM BESSEL OBS/FG - 0.333
14:13:35 8/11/86
LATITUDE
LONGITUDE
50.0
45.0
40.0
35.0
30.0
-92.5
-87.5
-82.5
-77.5
-72.5
-67.5
-62.5

(c)

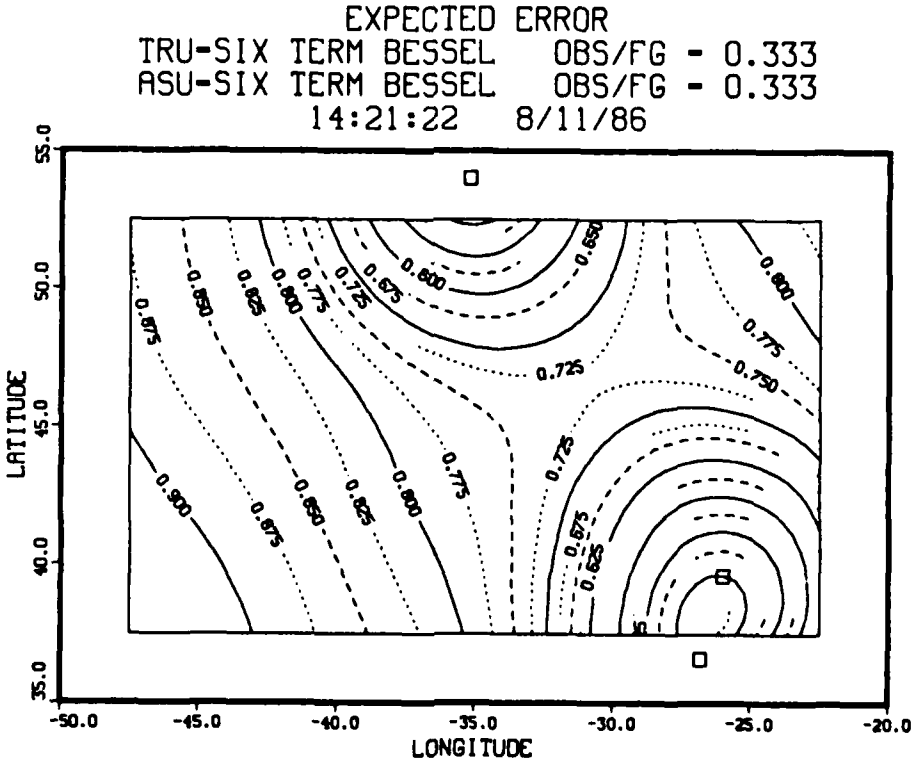
EXPECTED ERROR
TRU-SIX TERM BESSEL OBS/FG - 0.333
ASU-SIX TERM BESSEL OBS/FG - 0.333
14:21:22 8/11/86
LATITUDE
LONGITUDE
55.0
50.0
45.0
40.0
35.0
-50.0
-45.0
-40.0
-35.0
-30.0
-25.0
-20.0

(d)

FIGURE 2

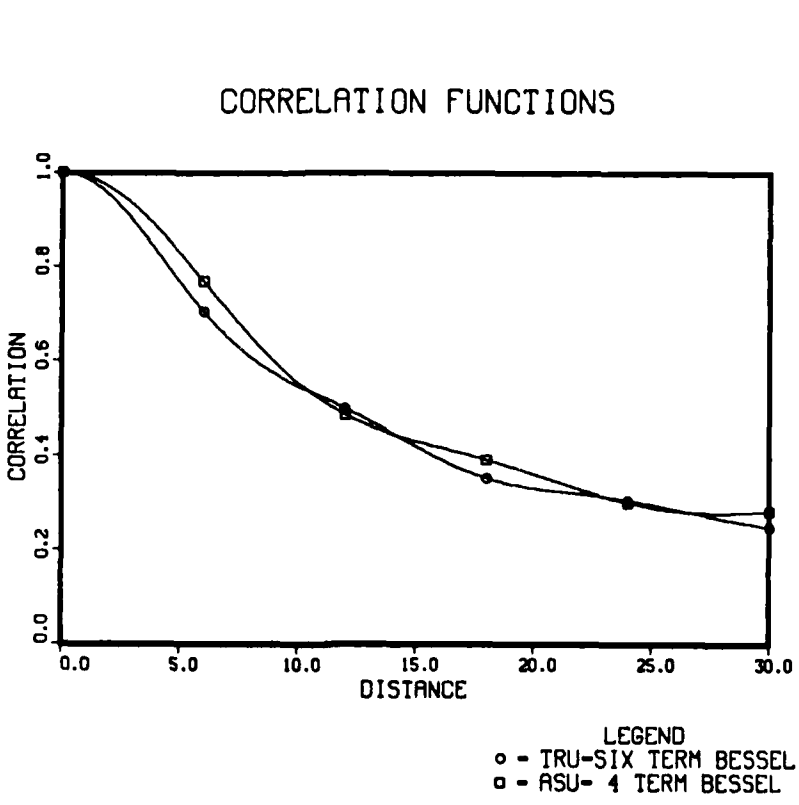
CORRELATION FUNCTIONS
CORRELATION
1.0
0.8
0.6
0.4
0.2
0.0
0.0
5.0
10.0
15.0
20.0
25.0
30.0
DISTANCE
LEGEND
o - TRU-SIX TERM BESSEL
□ - ASU- 4 TERM BESSEL

(a)

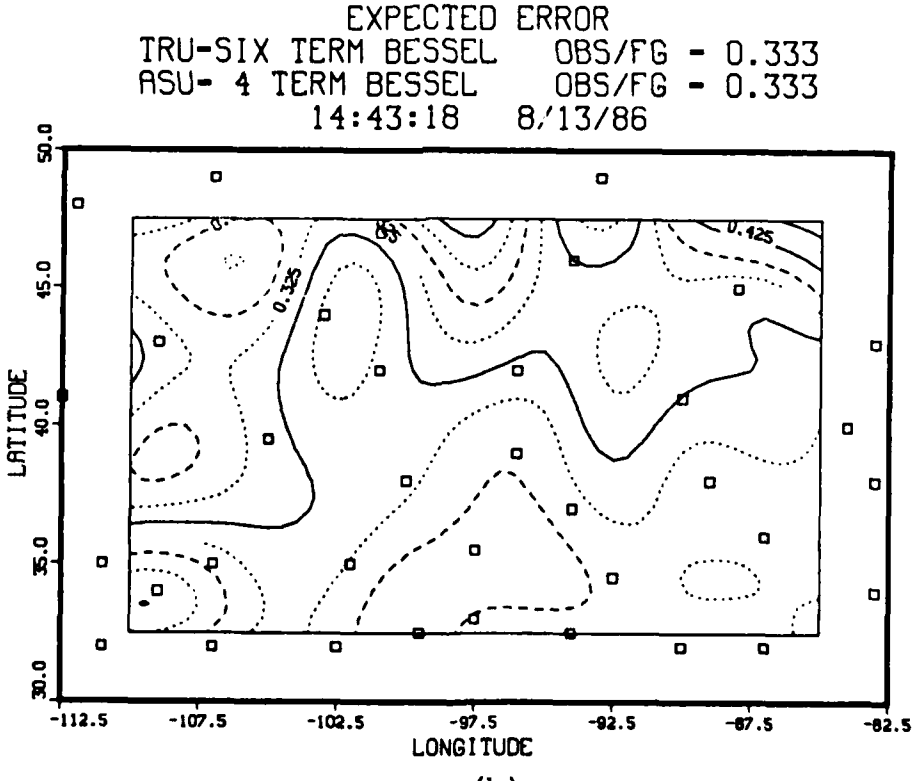
EXPECTED ERROR
TRU-SIX TERM BESSEL OBS/FG - 0.333
ASU- 4 TERM BESSEL OBS/FG - 0.333
14:43:18 8/13/86
LATITUDE
50.0
45.0
40.0
35.0
30.0
-112.5
-107.5
-102.5
-97.5
-92.5
-87.5
-82.5
LONGITUDE

(b)

FIGURE 3

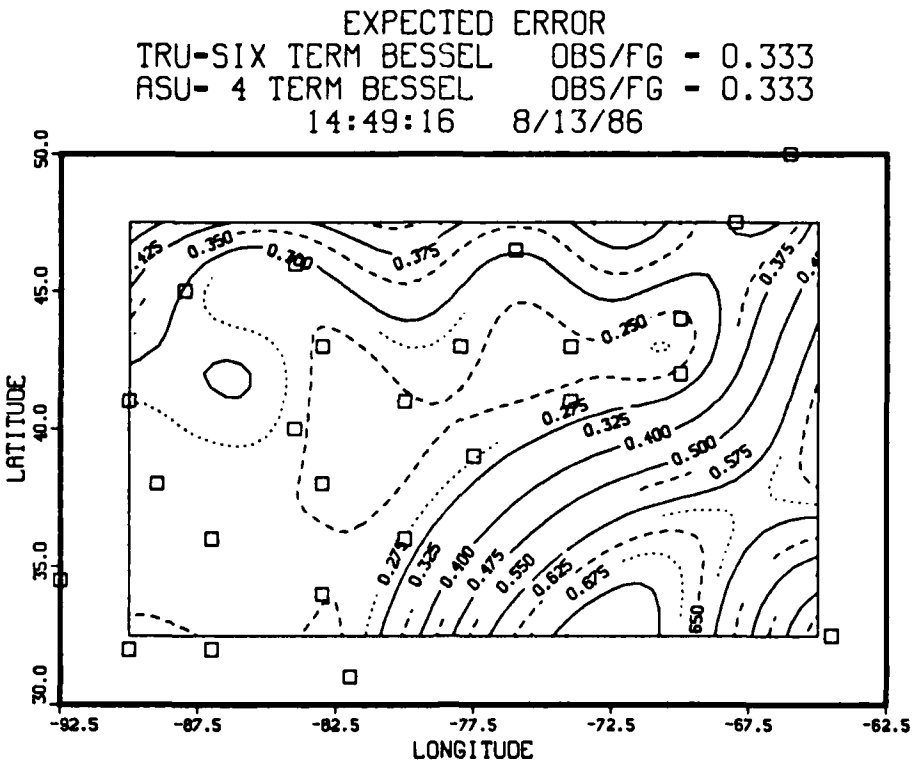
EXPECTED ERROR
TRU-SIX TERM BESSEL OBS/FG - 0.333
ASU- 4 TERM BESSEL OBS/FG - 0.333
14:49:16 8/13/86
LATITUDE
LONGITUDE
50.0
45.0
40.0
35.0
30.0
-92.5
-87.5
-82.5
-77.5
-72.5
-67.5
-62.5

(c)

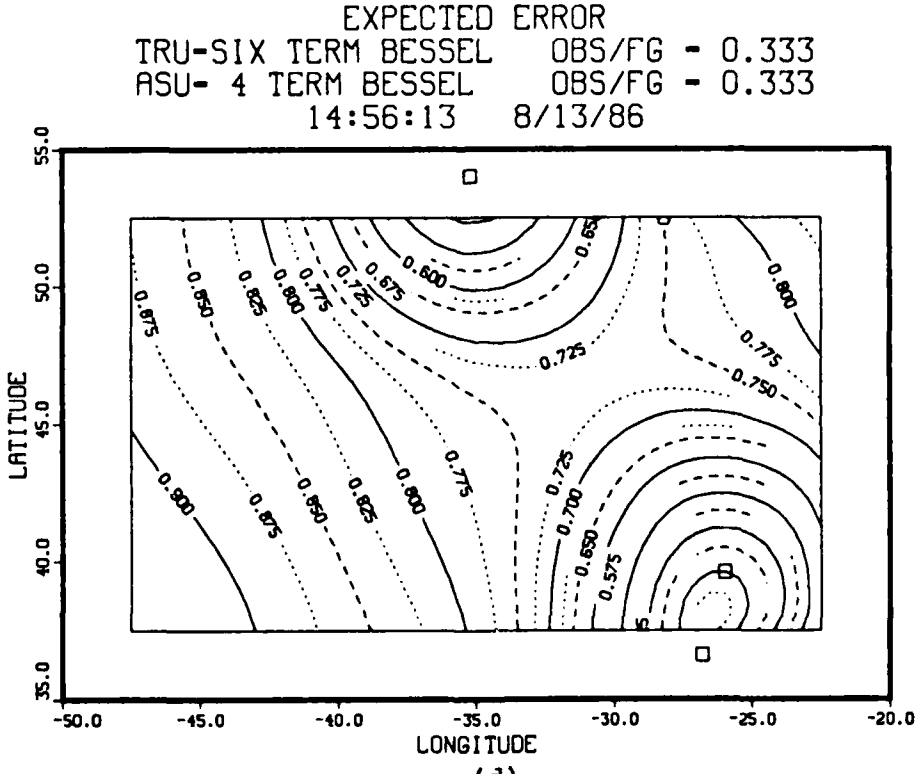
EXPECTED ERROR
TRU-SIX TERM BESSEL OBS/FG - 0.333
ASU- 4 TERM BESSEL OBS/FG - 0.333
14:56:13 8/13/86
LATITUDE
LONGITUDE
55.0
50.0
45.0
40.0
35.0
-50.0
-45.0
-40.0
-35.0
-30.0
-25.0
-20.0

(d)

FIGURE 3

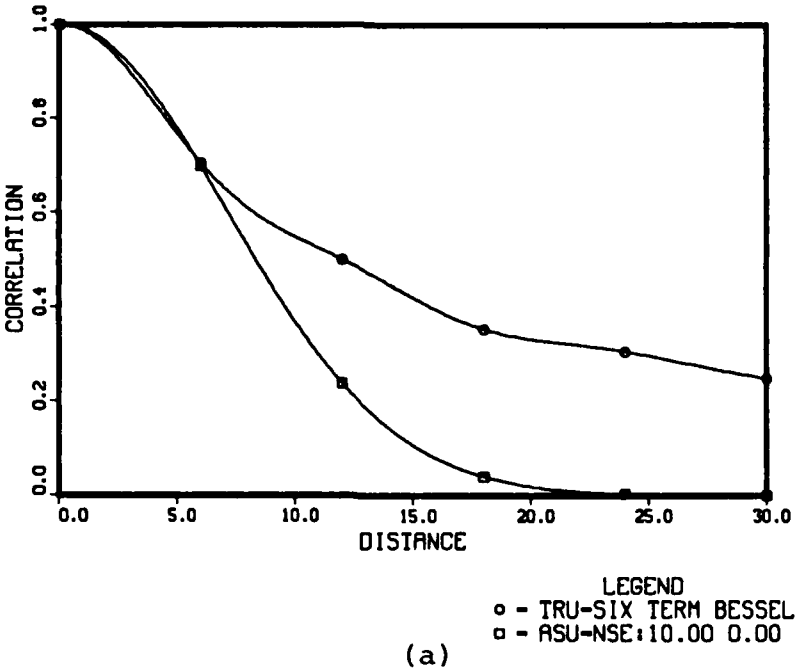
CORRELATION FUNCTIONS
CORRELATION
1.0
0.8
0.6
0.4
0.2
0.0
0.0
5.0
10.0
15.0
20.0
25.0
30.0
DISTANCE
LEGEND
o - TRU-SIX TERM BESSEL
□ - ASU-NSE:10.00 0.00

(a)

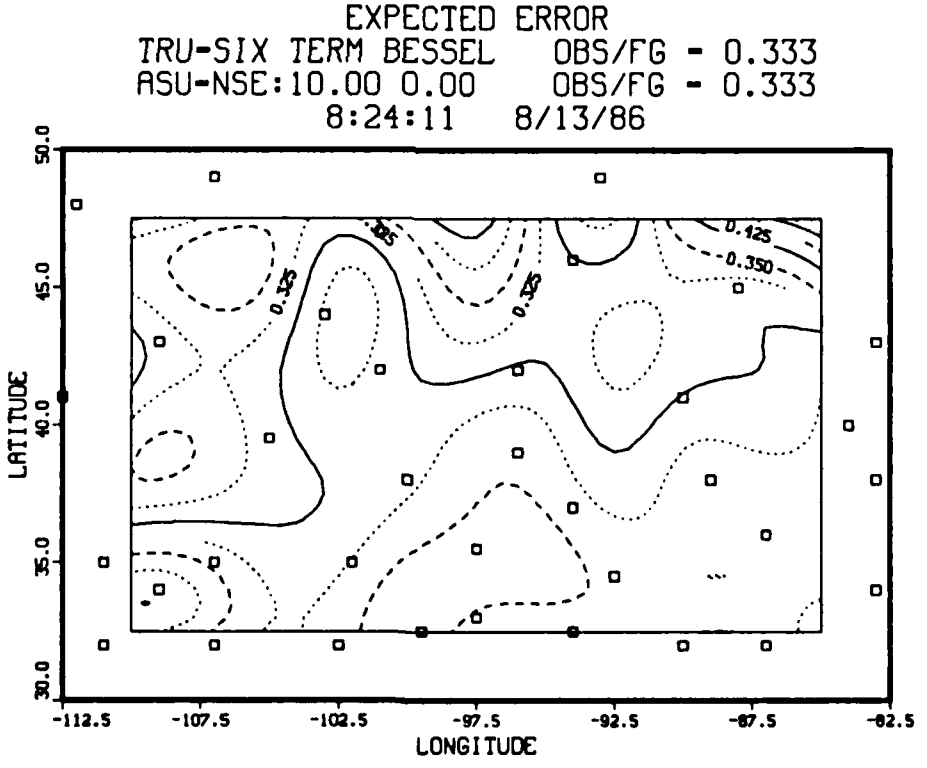
EXPECTED ERROR
TRU-SIX TERM BESSEL OBS/FG - 0.333
ASU-NSE:10.00 0.00 OBS/FG - 0.333
8:24:11 8/13/86
LATITUDE
50.0
45.0
40.0
35.0
30.0
-112.5
-107.5
-102.5
-97.5
-92.5
-87.5
-82.5
LONGITUDE
0.125
0.350

(b)

FIGURE 4

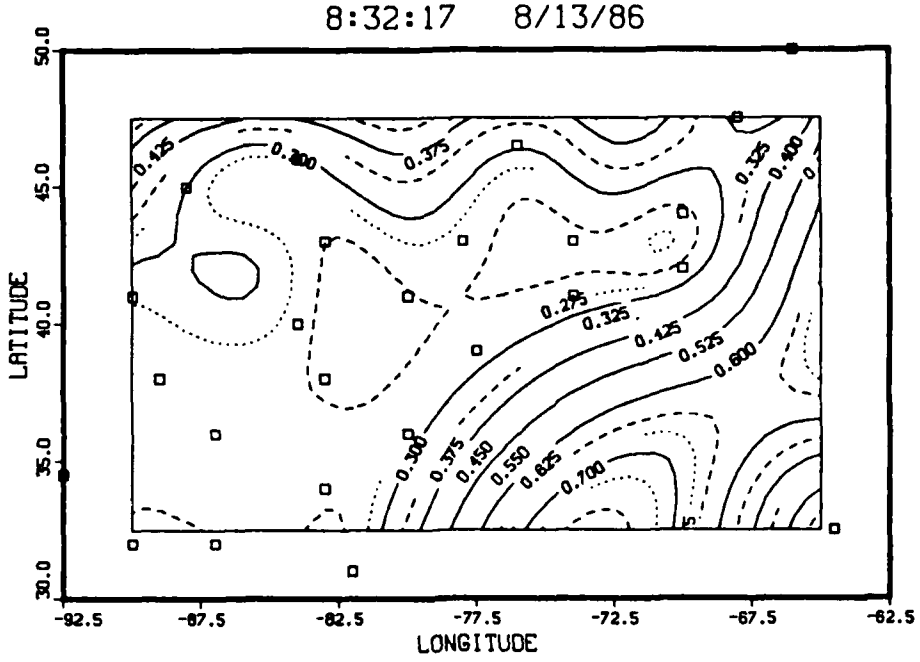
EXPECTED ERROR
TRU-SIX TERM BESSEL OBS/FG - 0.333
ASU-NSE:10.00 0.00 OBS/FG - 0.333
8:32:17 8/13/86
LATITUDE
LONGITUDE
50.0
45.0
40.0
35.0
30.0
-92.5
-87.5
-82.5
-77.5
-72.5
-67.5
-62.5

(c)

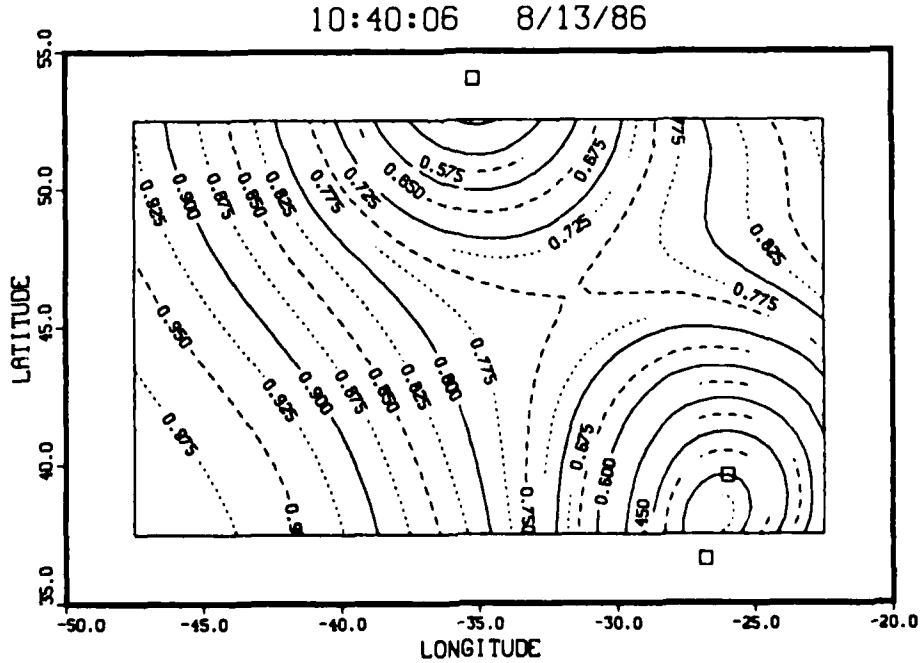
EXPECTED ERROR
TRU-SIX TERM BESSEL OBS/FG - 0.333
ASU-NSE:10.00 0.00 OBS/FG - 0.333
10:40:06 8/13/86
LATITUDE
LONGITUDE
55.0
50.0
45.0
40.0
35.0
-50.0
-45.0
-40.0
-35.0
-30.0
-25.0
-20.0

(d)

FIGURE 4

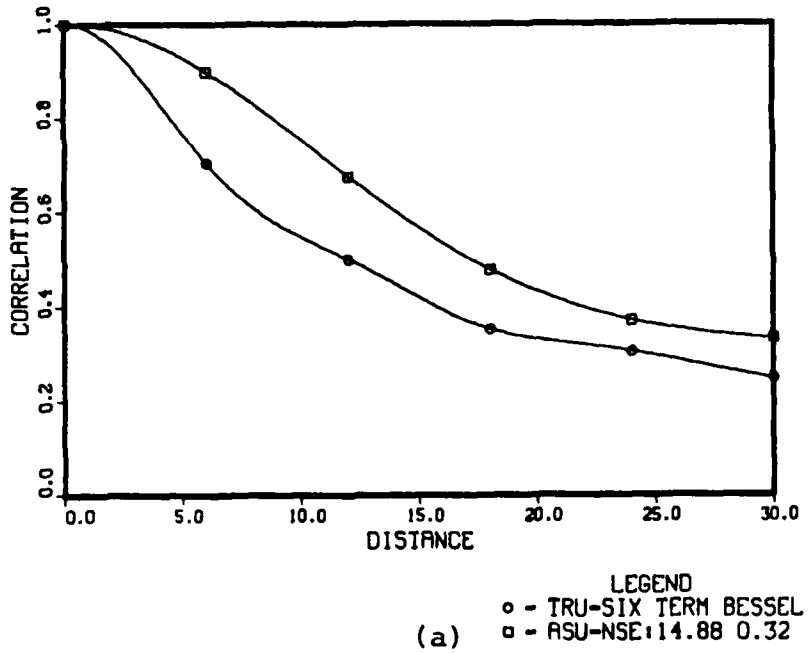
CORRELATION FUNCTIONS
CORRELATION
1.0
0.8
0.6
0.4
0.2
0.0
0.0
5.0
10.0
15.0
20.0
25.0
30.0
DISTANCE
LEGEND
o - TRU-SIX TERM BESSEL
□ - ASU-NSE:14.88 0.32

(a)

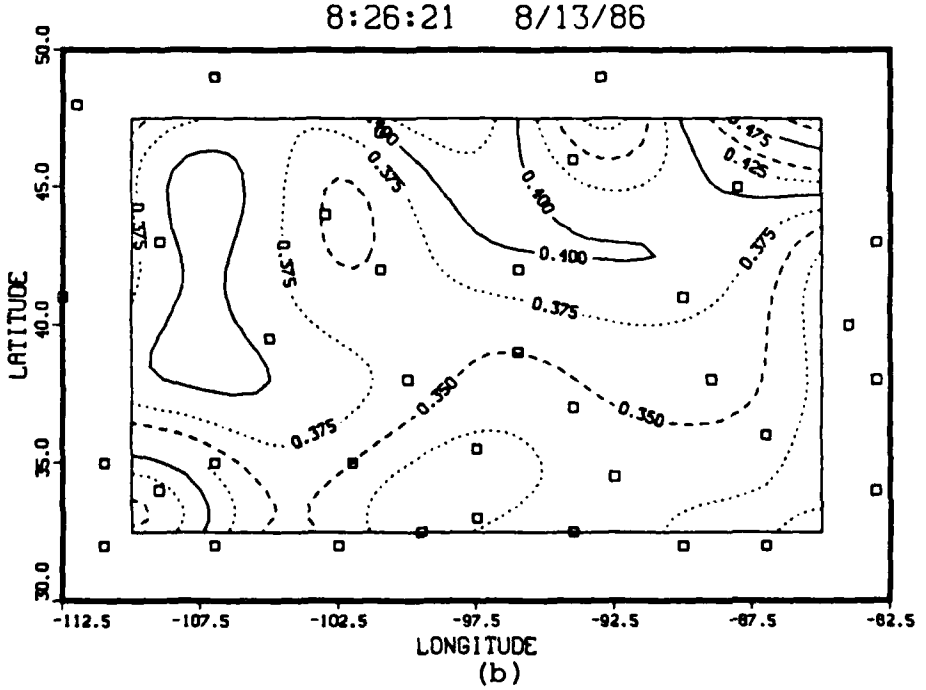
EXPECTED ERROR
TRU-SIX TERM BESSEL OBS/FG - 0.333
ASU-NSE:14.88 0.32 OBS/FG - 0.333
8:26:21 8/13/86
LATITUDE
50.0
45.0
40.0
35.0
30.0
-112.5
-107.5
-102.5
-97.5
-92.5
-87.5
-82.5
LONGITUDE
0.400
0.375
0.350
0.175
0.125

(b)

FIGURE 5

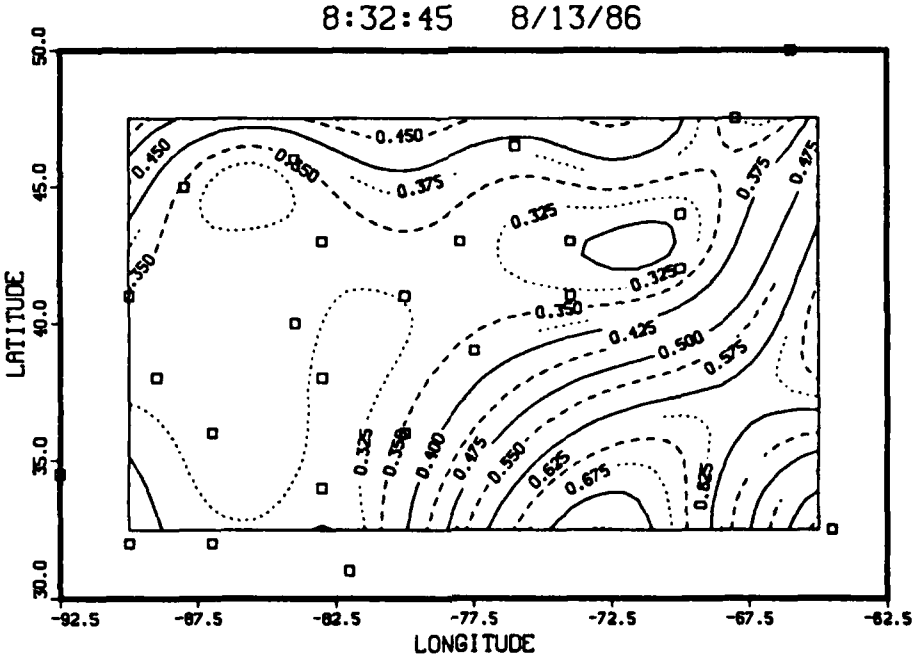
EXPECTED ERROR
TRU-SIX TERM BESSEL OBS/FG - 0.333
ASU-NSE:14.88 0.32 OBS/FG - 0.333
8:32:45 8/13/86
LATITUDE
LONGITUDE
50.0
45.0
40.0
35.0
30.0
-92.5
-87.5
-82.5
-77.5
-72.5
-67.5
-62.5

(c)

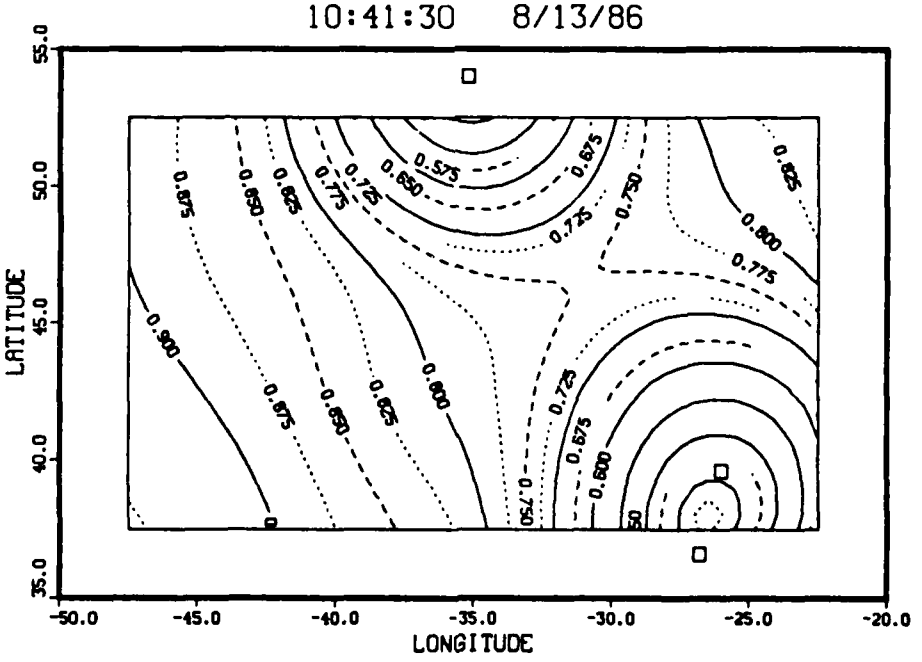
EXPECTED ERROR
TRU-SIX TERM BESSEL OBS/FG - 0.333
ASU-NSE:14.88 0.32 OBS/FG - 0.333
10:41:30 8/13/86
LATITUDE
LONGITUDE
55.0
50.0
45.0
40.0
35.0
-50.0
-45.0
-40.0
-35.0
-30.0
-25.0
-20.0

(d)

FIGURE 5

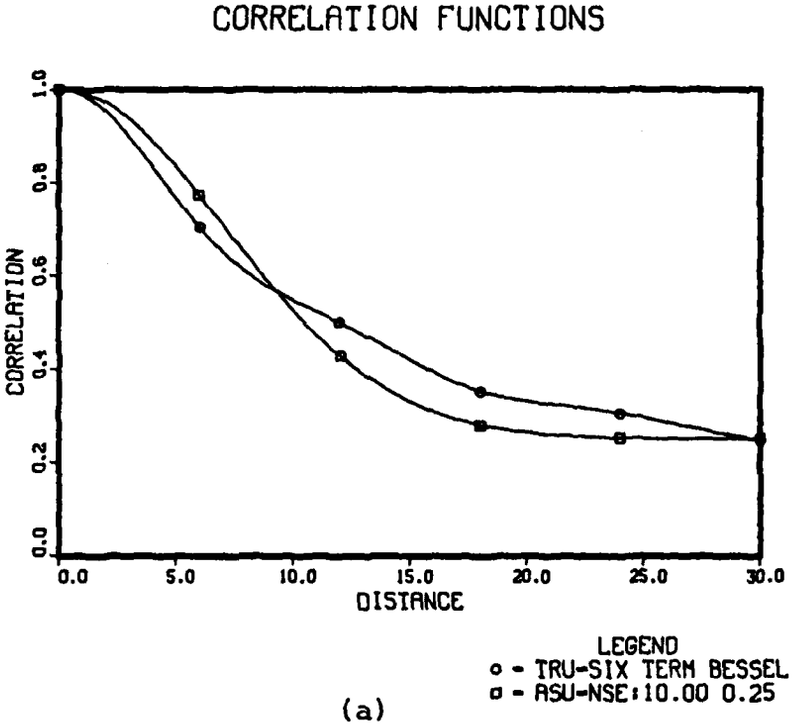
CORRELATION FUNCTIONS
CORRELATION
1.0
0.8
0.6
0.4
0.2
0.0
0.0
5.0
10.0
15.0
20.0
25.0
30.0
DISTANCE
LEGEND
o - TRU-SIX TERM BESSEL
□ - ASU-NSE:10.00 0.25

(a)

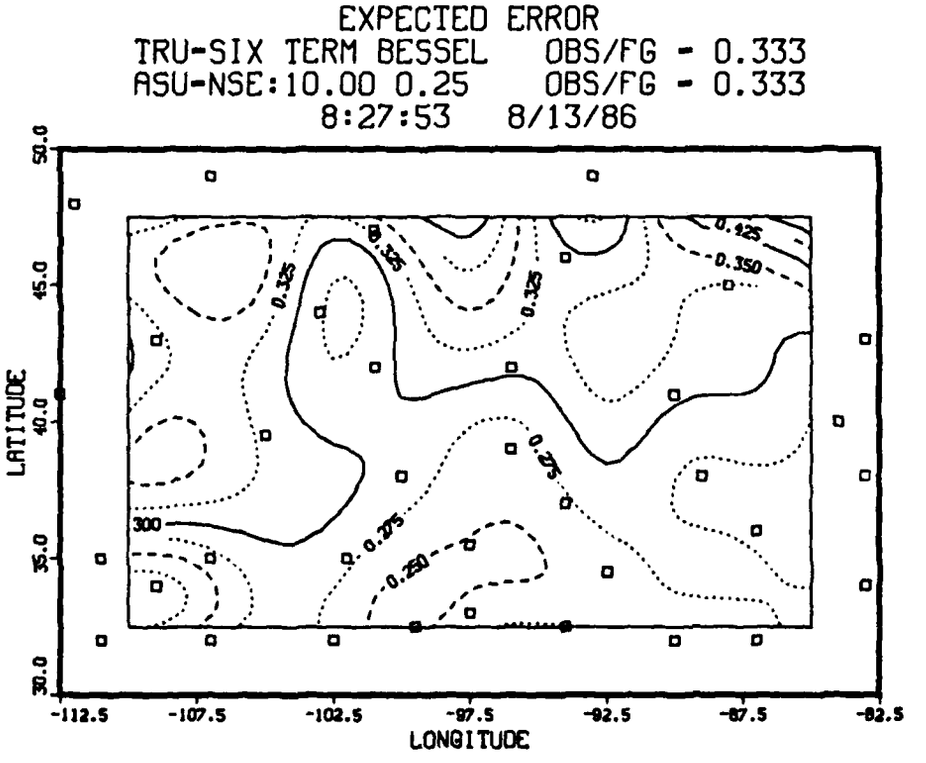
EXPECTED ERROR
TRU-SIX TERM BESSEL OBS/FG - 0.333
ASU-NSE:10.00 0.25 OBS/FG - 0.333
8:27:53 8/13/86
LATITUDE
50.0
45.0
40.0
35.0
30.0
-112.5
-107.5
-102.5
-97.5
-92.5
-87.5
-82.5
LONGITUDE
0.325
0.350
0.300
0.275
0.250

(b)

FIGURE 6

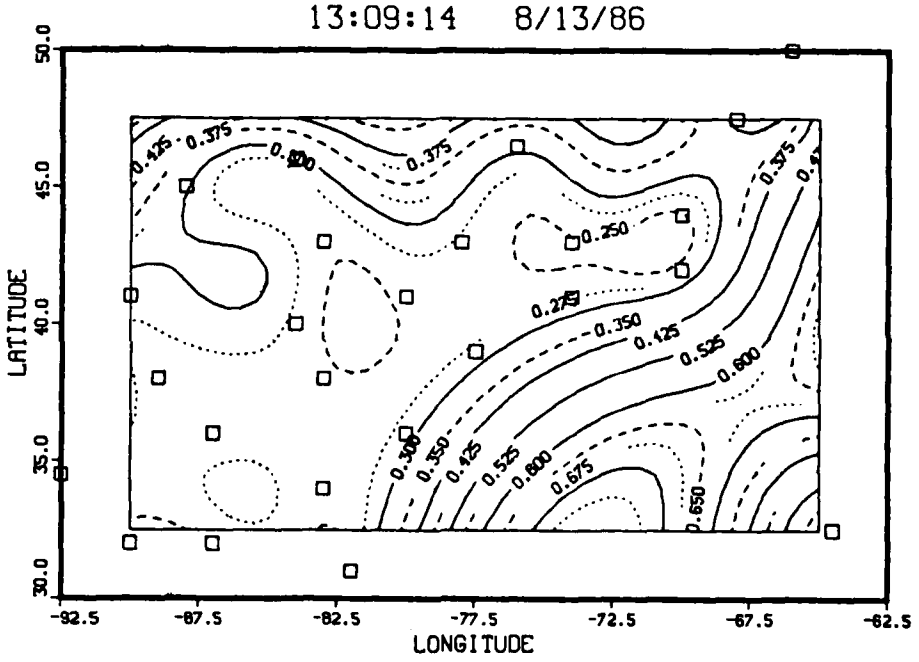
EXPECTED ERROR
TRU-SIX TERM BESSEL OBS/FG - 0.333
ASU-NSE:10.00 0.25 OBS/FG - 0.333
13:09:14 8/13/86
LATITUDE
LONGITUDE
50.0
45.0
40.0
35.0
30.0
-92.5
-87.5
-82.5
-77.5
-72.5
-67.5
-62.5

(c)

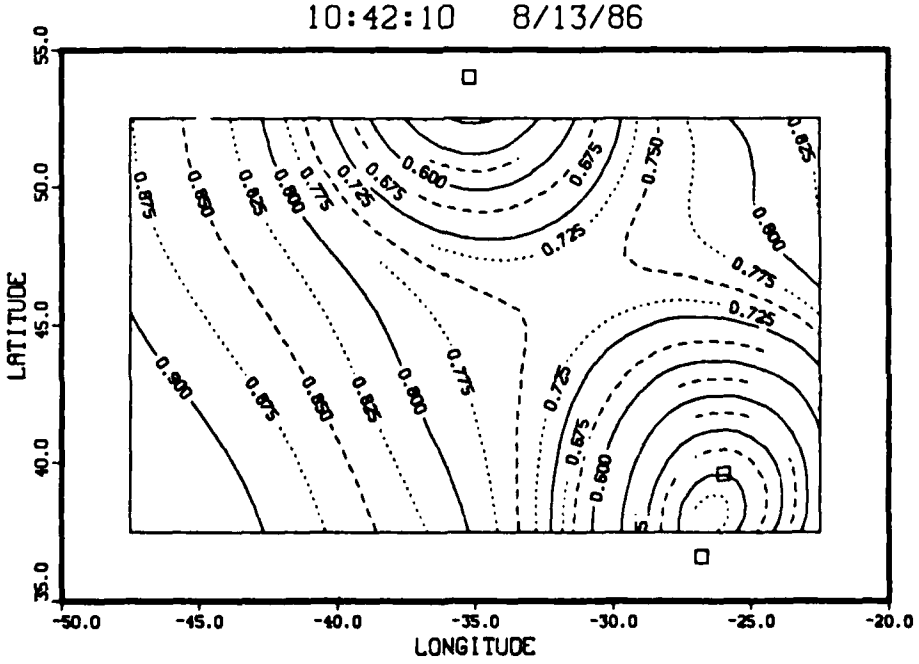
EXPECTED ERROR
TRU-SIX TERM BESSEL OBS/FG - 0.333
ASU-NSE:10.00 0.25 OBS/FG - 0.333
10:42:10 8/13/86
LATITUDE
LONGITUDE
55.0
50.0
45.0
40.0
35.0
-50.0
-45.0
-40.0
-35.0
-30.0
-25.0
-20.0

(d)

FIGURE 6

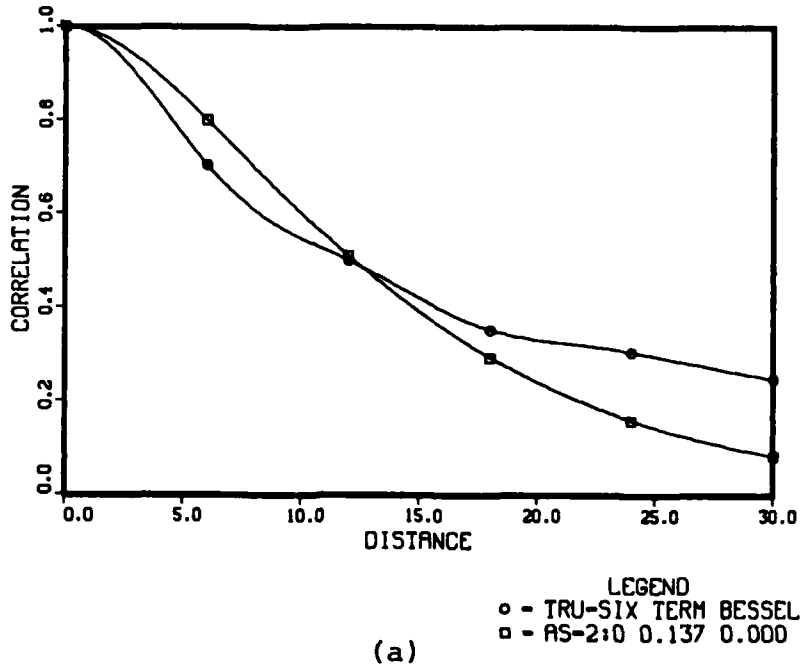
CORRELATION FUNCTIONS
CORRELATION
1.0
0.8
0.6
0.4
0.2
0.0
0.0
5.0
10.0
15.0
20.0
25.0
30.0
DISTANCE
LEGEND
o - TRU-SIX TERM BESSEL
□ - AS-2:0 0.137 0.000

(a)

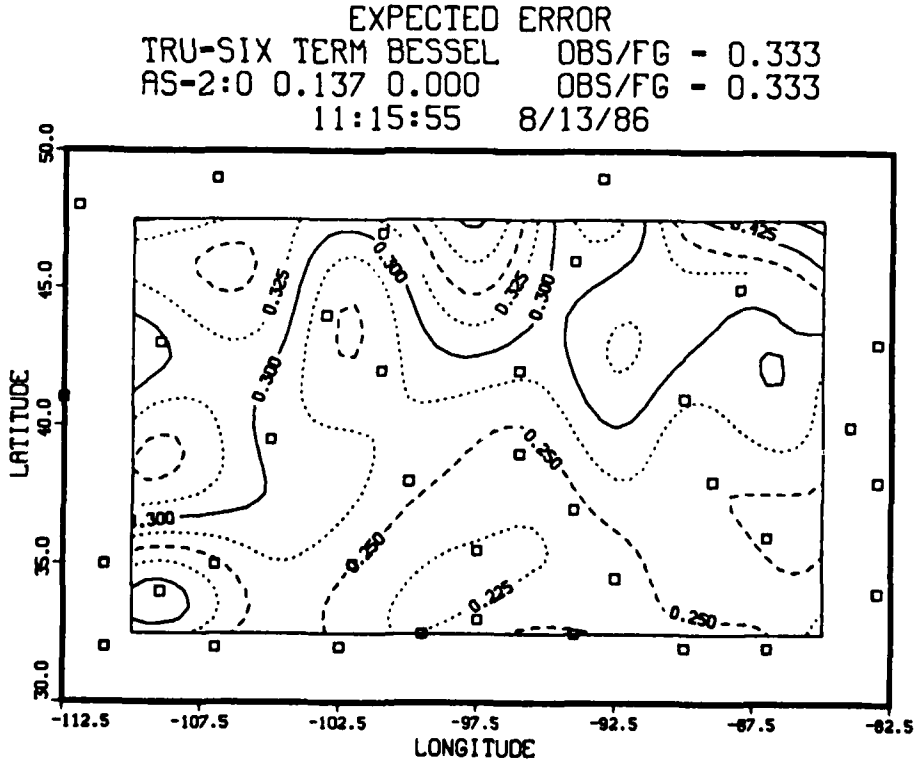
EXPECTED ERROR
TRU-SIX TERM BESSEL OBS/FG - 0.333
AS-2:0 0.137 0.000 OBS/FG - 0.333
11:15:55 8/13/86
LATITUDE
50.0
45.0
40.0
35.0
30.0
-112.5
-107.5
-102.5
-97.5
-92.5
-87.5
-82.5
LONGITUDE
0.325
0.300
0.275
0.250
0.225

(b)

FIGURE 7

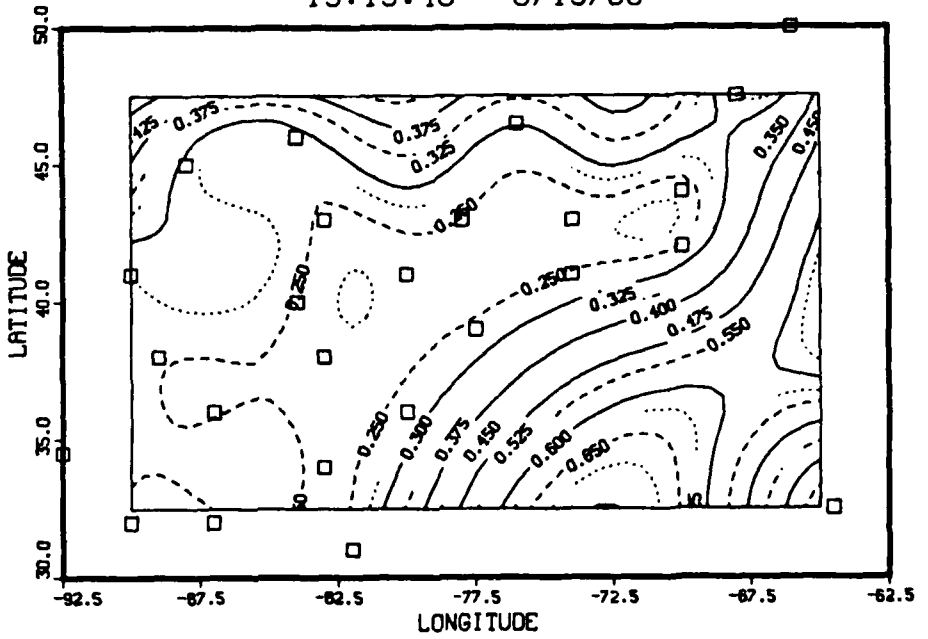
EXPECTED ERROR
TRU-SIX TERM BESSEL OBS/FG - 0.333
AS-2:0 0.137 0.000 OBS/FG - 0.333
13:19:46 8/13/86
LATITUDE
LONGITUDE
50.0
45.0
40.0
35.0
30.0
-92.5
-87.5
-82.5
-77.5
-72.5
-67.5
-62.5

(c)

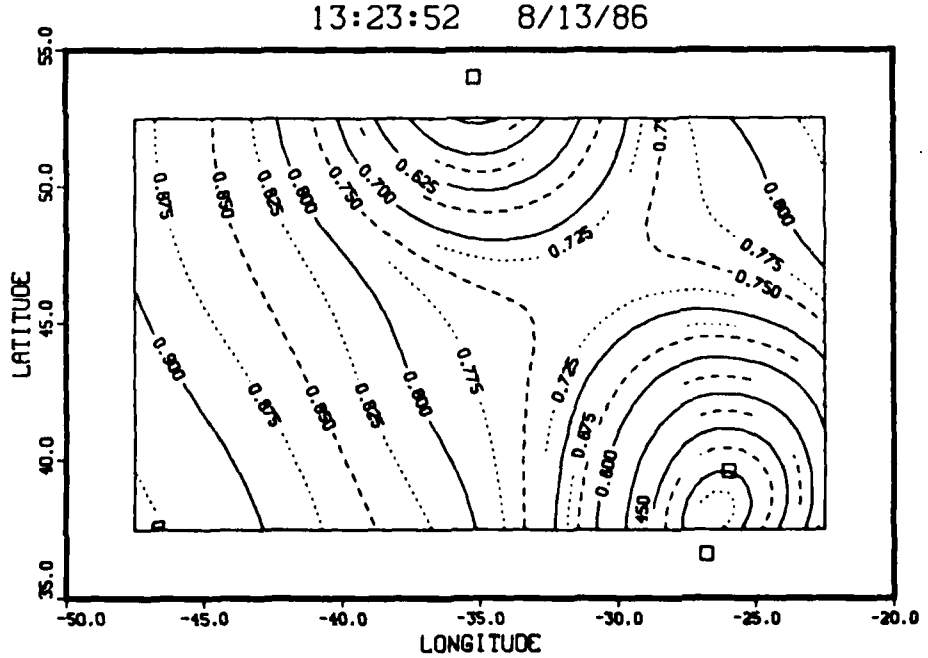
EXPECTED ERROR
TRU-SIX TERM BESSEL OBS/FG - 0.333
AS-2:0 0.137 0.000 OBS/FG - 0.333
13:23:52 8/13/86
LATITUDE
LONGITUDE
55.0
50.0
45.0
40.0
35.0
-50.0
-45.0
-40.0
-35.0
-30.0
-25.0
-20.0

(d)

FIGURE 7

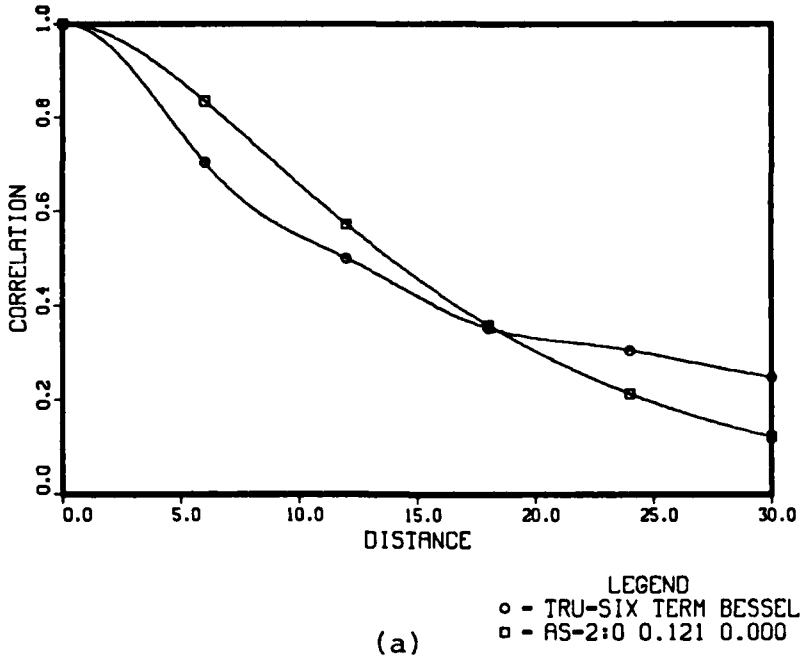
CORRELATION FUNCTIONS
CORRELATION
1.0
0.8
0.6
0.4
0.2
0.0
0.0
5.0
10.0
15.0
20.0
25.0
30.0
DISTANCE
LEGEND
o - TRU-SIX TERM BESSEL
□ - AS-2:0 0.121 0.000

(a)

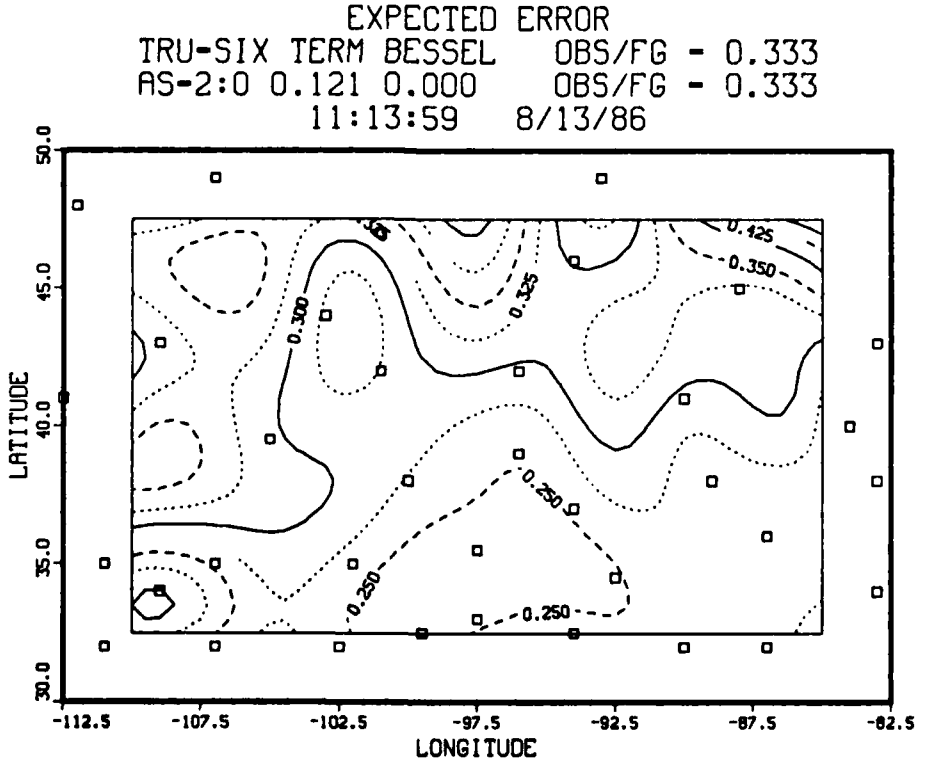
EXPECTED ERROR
TRU-SIX TERM BESSEL OBS/FG - 0.333
AS-2:0 0.121 0.000 OBS/FG - 0.333
11:13:59 8/13/86
LATITUDE
50.0
45.0
40.0
35.0
30.0
-112.5
-107.5
-102.5
-97.5
-92.5
-87.5
-82.5
LONGITUDE
0.125
0.350
0.325
0.300
0.250
0.250
0.250

(b)

FIGURE 8

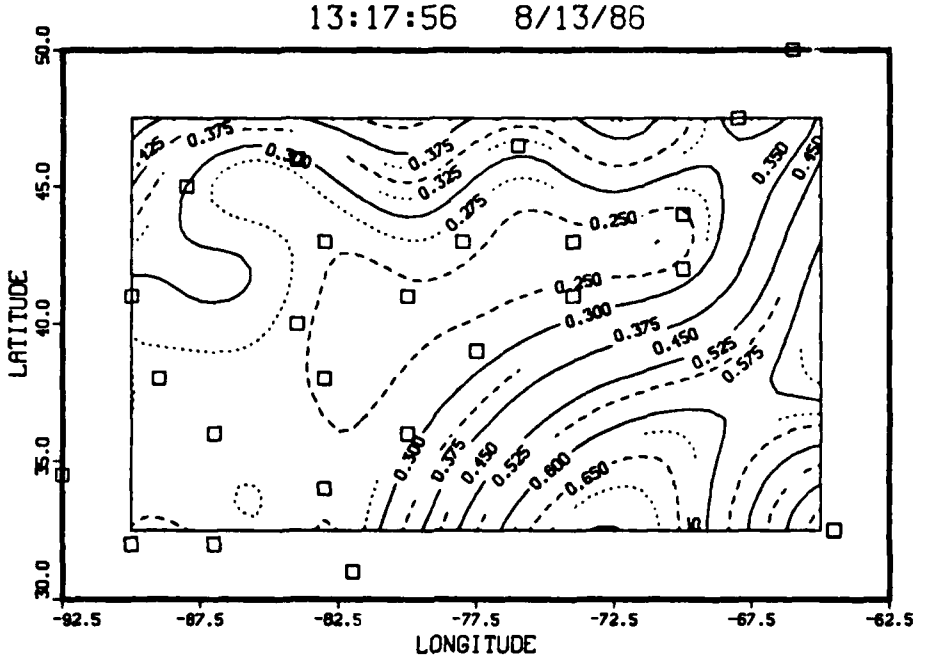
EXPECTED ERROR
TRU-SIX TERM BESSEL OBS/FG - 0.333
AS-2:0 0.121 0.000 OBS/FG - 0.333
13:17:56 8/13/86
LATITUDE
LONGITUDE
50.0
45.0
40.0
35.0
30.0
-92.5
-87.5
-82.5
-77.5
-72.5
-67.5
-62.5

(c)

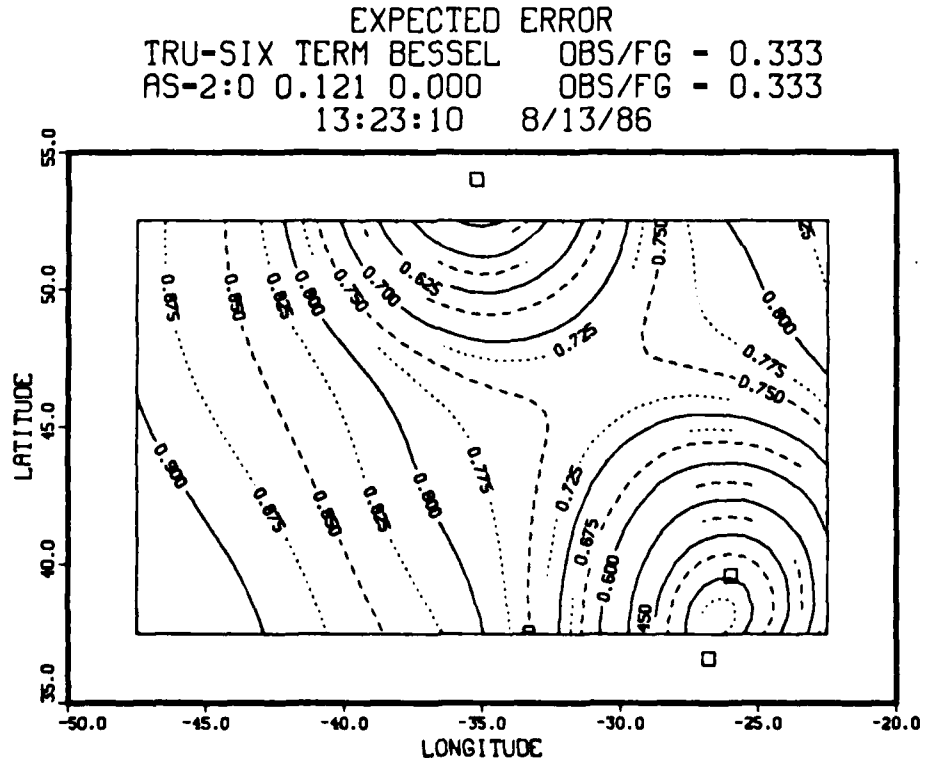
EXPECTED ERROR
TRU-SIX TERM BESSEL OBS/FG - 0.333
AS-2:0 0.121 0.000 OBS/FG - 0.333
13:23:10 8/13/86
LATITUDE
LONGITUDE
55.0
50.0
45.0
40.0
35.0
-50.0
-45.0
-40.0
-35.0
-30.0
-25.0
-20.0

(d)

FIGURE 8

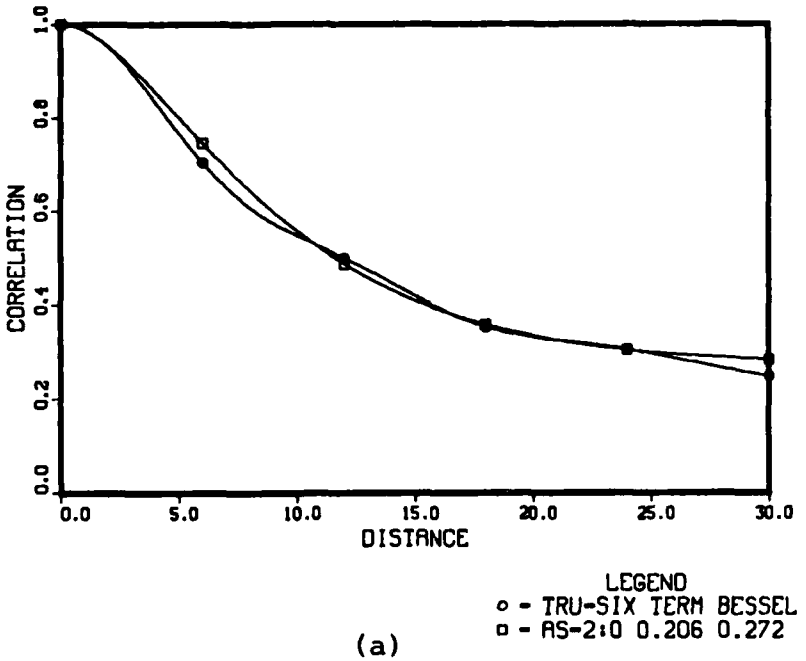
CORRELATION FUNCTIONS
CORRELATION
1.0
0.8
0.6
0.4
0.2
0.0
0.0
5.0
10.0
15.0
20.0
25.0
30.0
DISTANCE
LEGEND
o - TRU-SIX TERM BESSEL
□ - AS-2:0 0.206 0.272

(a)

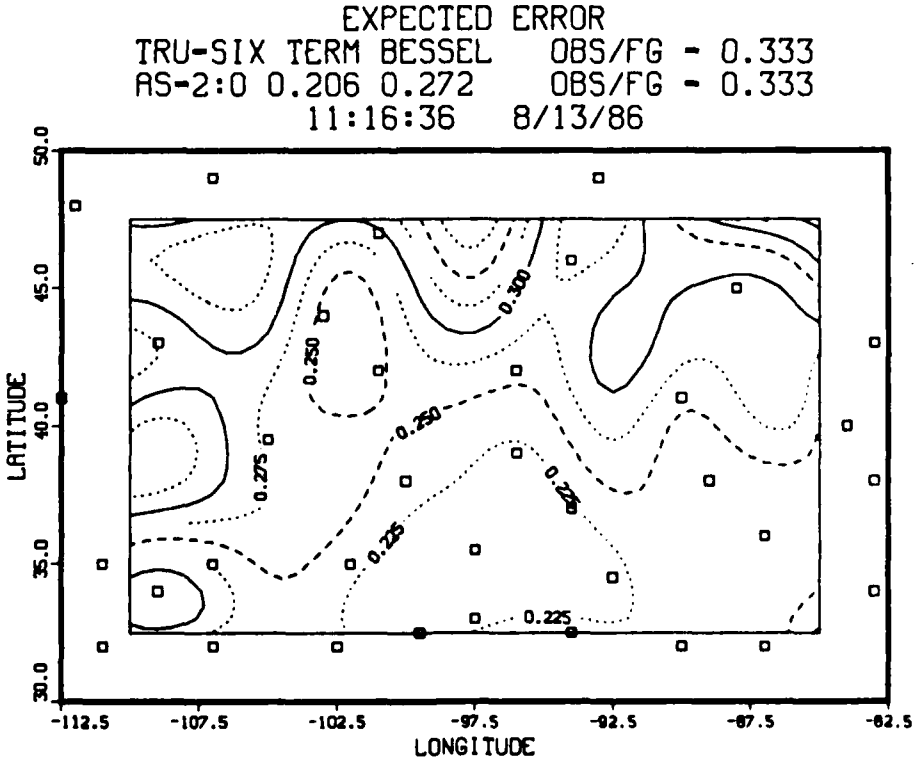
EXPECTED ERROR
TRU-SIX TERM BESSEL OBS/FG - 0.333
AS-2:0 0.206 0.272 OBS/FG - 0.333
11:16:36 8/13/86
LATITUDE
50.0
45.0
40.0
35.0
30.0
0.300
0.250
0.250
0.275
0.225
0.225
-112.5
-107.5
-102.5
-97.5
-92.5
-87.5
-82.5
LONGITUDE

(b)

FIGURE 9

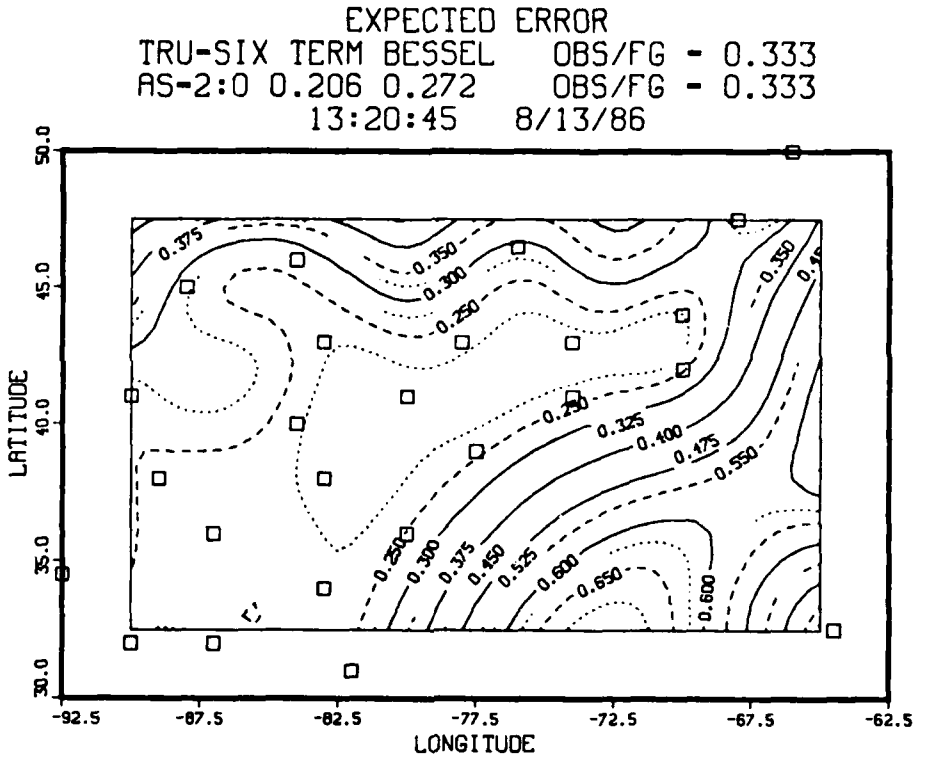
EXPECTED ERROR
TRU-SIX TERM BESSEL OBS/FG - 0.333
AS-2:0 0.206 0.272 OBS/FG - 0.333
13:20:45 8/13/86
LATITUDE
LONGITUDE
50.0
45.0
40.0
35.0
30.0
-92.5
-87.5
-82.5
-77.5
-72.5
-67.5
-62.5

(c)

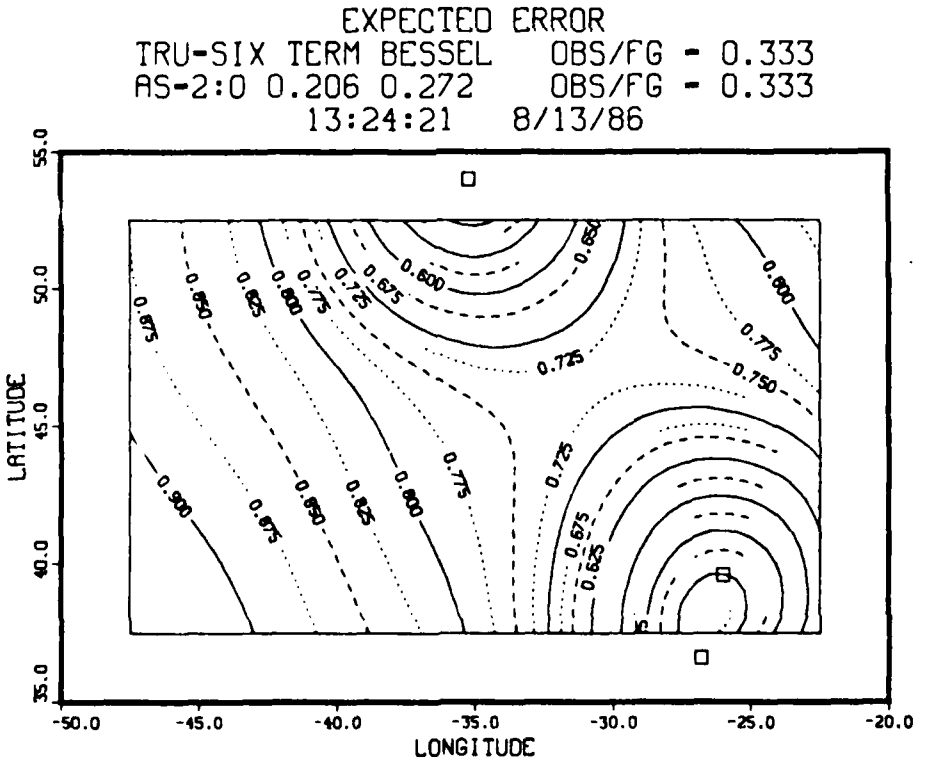
EXPECTED ERROR
TRU-SIX TERM BESSEL OBS/FG - 0.333
AS-2:0 0.206 0.272 OBS/FG - 0.333
13:24:21 8/13/86
LATITUDE
LONGITUDE
55.0
50.0
45.0
40.0
35.0
-50.0
-45.0
-40.0
-35.0
-30.0
-25.0
-20.0

(d)

FIGURE 9

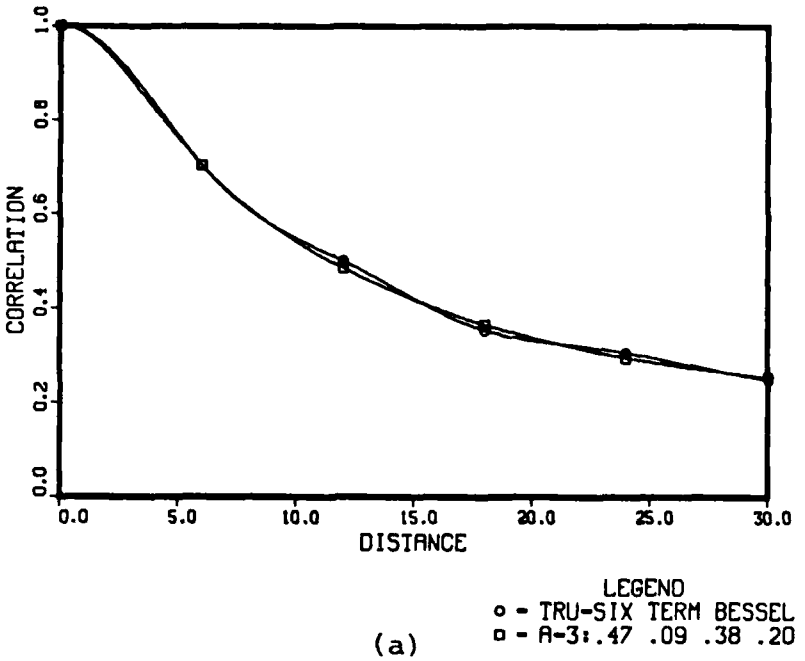
CORRELATION FUNCTIONS
CORRELATION
1.0
0.8
0.6
0.4
0.2
0.0
0.0
5.0
10.0
15.0
20.0
25.0
30.0
DISTANCE
LEGEND
o - TRU-SIX TERM BESSEL
□ - A-3:.47 .09 .38 .20

(a)

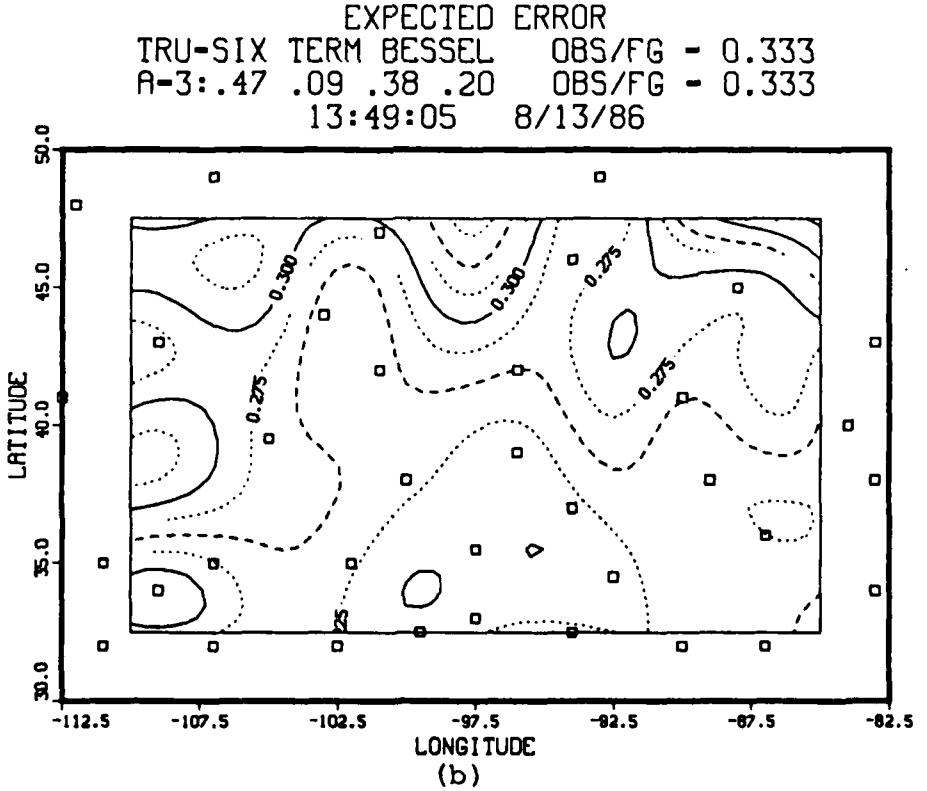
EXPECTED ERROR
TRU-SIX TERM BESSEL OBS/FG - 0.333
A-3:.47 .09 .38 .20 OBS/FG - 0.333
13:49:05 8/13/86
LATITUDE
50.0
45.0
40.0
35.0
30.0
0.300
0.300
0.275
0.275
0.275
-112.5
-107.5
-102.5
-97.5
-92.5
-87.5
-82.5
LONGITUDE

(b)

FIGURE 10

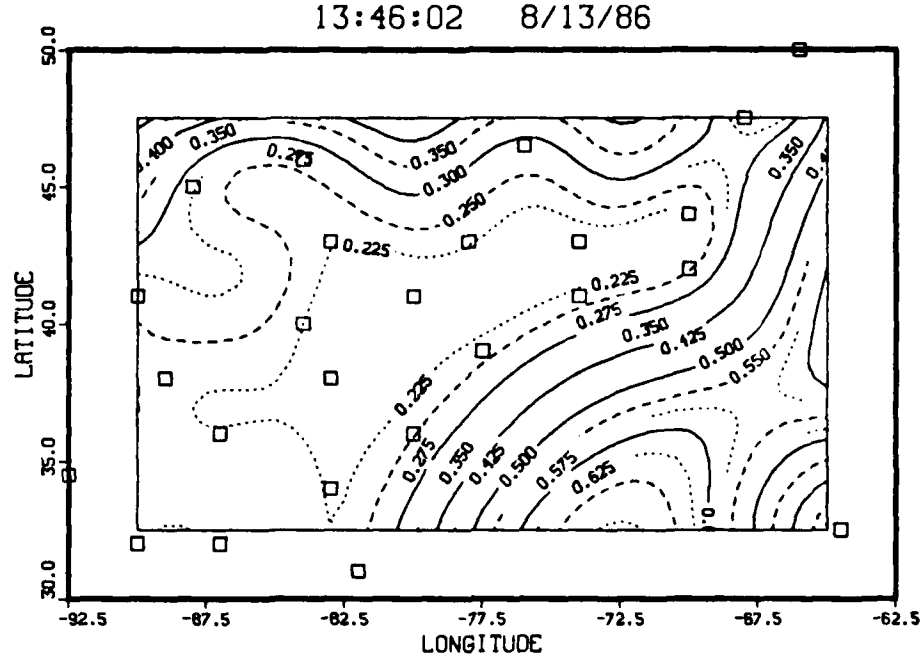
EXPECTED ERROR
TRU-SIX TERM BESSEL OBS/FG - 0.333
A-3:.47 .09 .38 .20 OBS/FG - 0.333
13:46:02 8/13/86
LATITUDE
LONGITUDE
50.0
45.0
40.0
35.0
30.0
-92.5
-87.5
-82.5
-77.5
-72.5
-67.5
-62.5

(c)

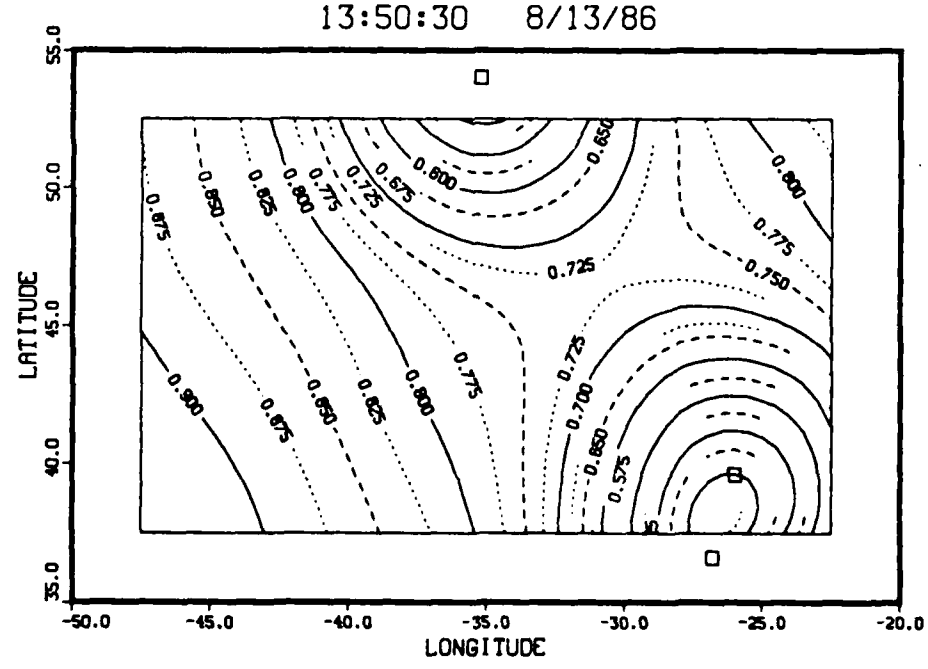
EXPECTED ERROR
TRU-SIX TERM BESSEL OBS/FG - 0.333
A-3:.47 .09 .38 .20 OBS/FG - 0.333
13:50:30 8/13/86
LATITUDE
LONGITUDE
55.0
50.0
45.0
40.0
35.0
-50.0
-45.0
-40.0
-35.0
-30.0
-25.0
-20.0

(d)

FIGURE 10

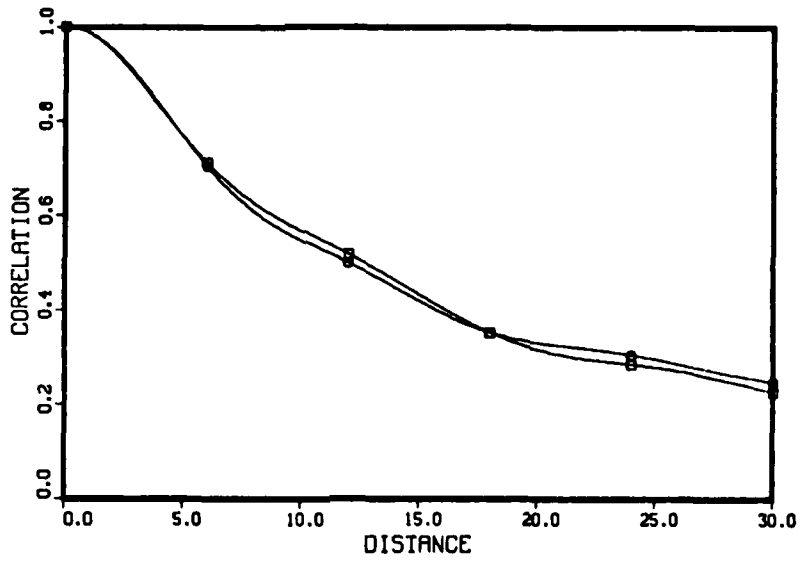
CORRELATION FUNCTIONS
CORRELATION
0.0
0.2
0.4
0.6
0.8
1.0
0.0
5.0
10.0
15.0
20.0
25.0
30.0
DISTANCE
LEGEND
o - TRU-SIX TERM BESSEL
o - A-DC.47 .14 .96 .5

(a)

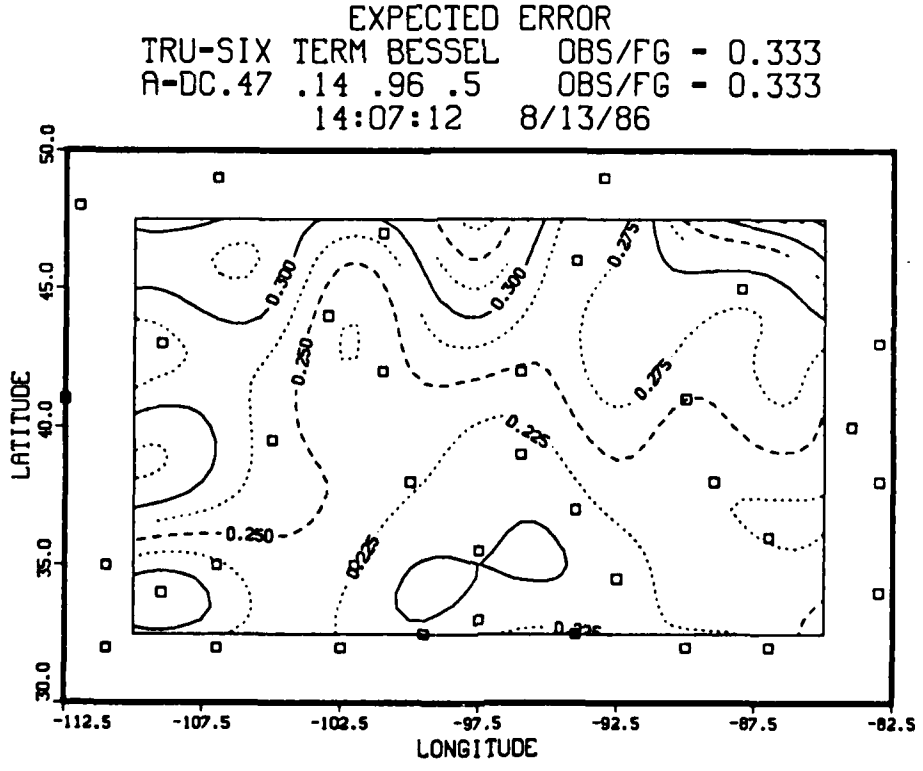
EXPECTED ERROR
TRU-SIX TERM BESSEL OBS/FG - 0.333
A-DC.47 .14 .96 .5 OBS/FG - 0.333
14:07:12 8/13/86
LATITUDE
50.0
45.0
40.0
35.0
30.0
0.300
0.250
0.275
0.225
-112.5
-107.5
-102.5
-97.5
-92.5
-87.5
-82.5
LONGITUDE

(b)

FIGURE 11

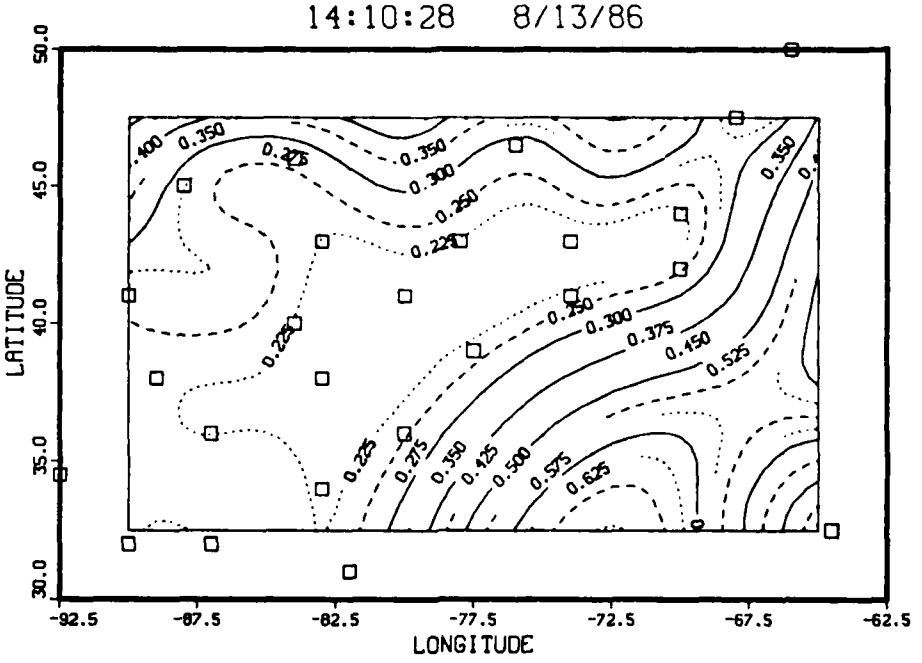
EXPECTED ERROR
TRU-SIX TERM BESSEL OBS/FG - 0.333
A-DC.47 .14 .96 .5 OBS/FG - 0.333
14:10:28 8/13/86
LATITUDE
LONGITUDE
50.0
45.0
40.0
35.0
30.0
-92.5
-87.5
-82.5
-77.5
-72.5
-67.5
-62.5

(c)

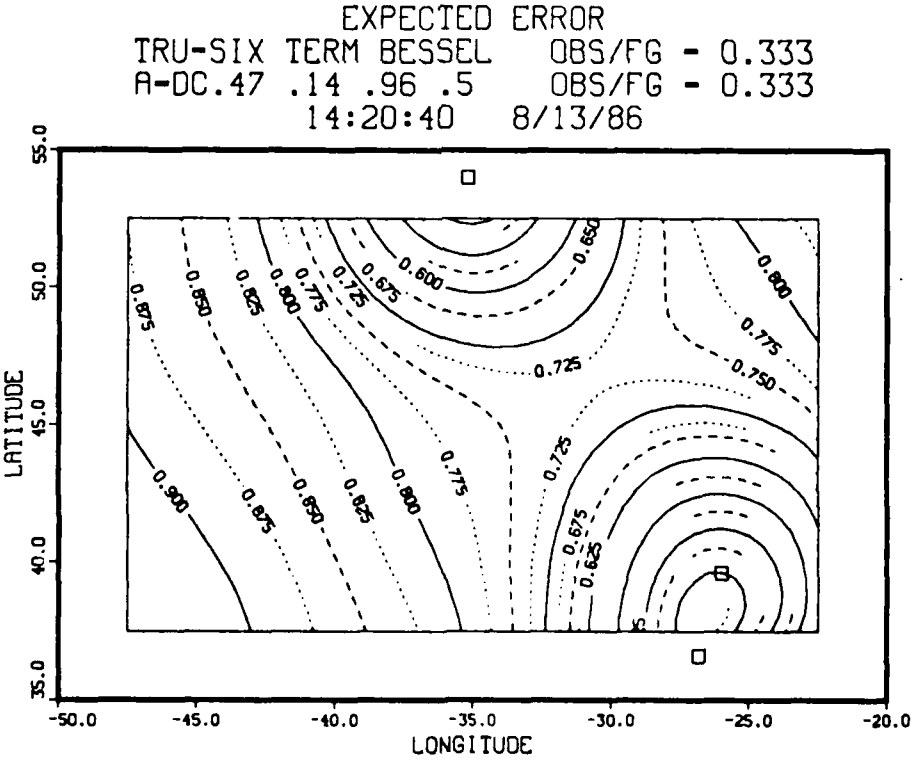
EXPECTED ERROR
TRU-SIX TERM BESSEL OBS/FG - 0.333
A-DC.47 .14 .96 .5 OBS/FG - 0.333
14:20:40 8/13/86
LATITUDE
LONGITUDE
55.0
50.0
45.0
40.0
35.0
-50.0
-45.0
-40.0
-35.0
-30.0
-25.0
-20.0

(d)

FIGURE 11

Appendix 1

This appendix lists many of the functions proposed for use as correlation functions in SI during the past 15 or 20 years. Many have been mentioned by several authors, and there does not seem to be any standard notation for parameters. This listing will attempt to be somewhat consistent in the meaning of various parameter symbols used in defining the functions. Of course, this kind of goal cannot be completely successful, and it is not in this case. In addition, the attempt results in possible confusion in certain cases where the role of symbols used in the cited literature is interchanged with that adopted here. Nonetheless, it seemed to be useful to try to be consistent, although reasonable persons can certainly disagree on what that means.

The symbols used in this compendium have meanings as described here.

a	- oscillation parameter
b	- decay parameter (primary or one in oscillatory term)
c,d,e	- other nonlinear parameters
A, A_i	- linear coefficients
s	- distance, assumed positive to ensure symmetry

Finally, while the list is extensive, no claim is made that it is exhaustive or complete. Apologies are made in advance to those authors whose suggestion of any of one of the below predated all the references.

	Function	References
1.	$e^{-(s/b)^2}$	Bergman (1979) Buell (1972) Gandin (1963) Lorenc (1981) McPherson (1982) Seaman & Hutchinson (1985) Schlatter, et.al. (1976) Thiébaux (1976)
2.	$(1-A)e^{-(s/b)^2} + A$	Thiébaux, et.al. (1985)
3.	$(1 + \sum_i A_i s^i)e^{-(s/b)^2}$	Buell (1972)
4.	$\cos(as)e^{-bs}$	Creutin & Obled (1982)
5.	$[A + (1-A)\cos(as)]e^{-bs}$	Seaman & Hutchinson (1985)
6.	$(1 + bs)e^{-bs}$	Buell (1972) Seaman & Hutchinson (1985) Thiébaux, et.al. (1985) Yudin (1961)
7.	$[\cos(as) + (b/a)\sin(as)]e^{-bs}$	Thiébaux (1985)
8.	$A+(1-A)[\cos(as)+(b/a)\sin(as)]e^{-bs}$	Thiébaux, et.al. (1985)
9.	$[\bar{a}\cos(as)+\bar{b}\sin(as)]e^{-bs}+\bar{c}e^{-cs}$ * $(\bar{a},\bar{b},\bar{c}) = G(a,b,c)$	Thiébaux, et.al. (1985)
10.	$A+(1-A)[\bar{a}\cos(as)+\bar{b}\sin(as)]e^{-bs}+\bar{c}e^{-cs}]$ * $(\bar{a},\bar{b},\bar{c}) = G(a,b,c)$	Thiébaux, et.al. (1985)
11.	$[A + (1-A)e^{-bs^c}\cos(as)$	Alaka & Alvander (1972) Steinitz, et.al. (1971)
12.	$[A + (1-A)\cos(as)](1 + (bs)^2)^{-c}$	Seaman & Hutchinson (1985) Thiébaux (1976)
13.	$[A + (1-A)\cos(as)]e^{-bs^c}$	Thiébaux (1975)
14.	$[A + (1-A)J_0(as)]e^{-bs^c}$	Thiébaux (1975)
15.	$[A + (1+a)J_0(as](1 + (bs)^2)^{-c}$	Thiébaux (1975)
16.	$\sum_i A_i J_0(k_i s/R) + A_0$ R - radius k_i - ith root of J_0	Rutherford (1972) Lonnberg (1982)

18.	$(1 + (bs)^2)^{-c}$	Buell (1972)
19.	$(1 + cs + a(cs)^2)e^{-bs}$	Buell (1972)
20.	$\mathrm{sech}(bs)$	Buell (1972)
21.	$\sin(as)/(as)$	Buell (1972)
22.	$K_1(bs)/(bs)$	Buell (1972)
23.	$2^{1/3}\Gamma(2/3)(bs)^{2/3}K_{2/3}(bs)$	Buell (1972)
24.	$\frac{be^{-cs} - ce^{-bs}}{b - c}$	Buell (1972)

* $\bar{a} = (3b^2-a^2-c^2)ac/D$

$\bar{b} = (b^2-3a^2-c^2)bc/D$

$\bar{c} = -2(b^2+a^2)ab/D$

where $D = (3b^2-a^2-c^2ac-2(b^2+a^2)ab$

Appendix 2

This appendix contains the results of some experiments in generating simulated raw statistics for first-guess plus observation errors. In many respects the data appears very similar to that contained in the literature, e.g. Julian and Thiébaux (1975), Schlatter (1975), Thiébaux (1976), and Thiébaux, et.al. (1985). However, some interesting observations can be made when the simulations involve different sets of realizations, and especially when different numbers of realizations are involved.

First, it was desired to continue the use of the six term Bessel function as the model first-guess correlation function and to use the grid/observation set MUS as the basis for the simulation. This presented some difficulty, as the generation of first-guess errors at the grid points (9x13=117 of them) with the specified spatial error covariance function requires factoring the desired spatial covariance matrix into the form $A=LL^t$. This proved to be impossible to do because the matrix was very ill conditioned. Just a little "tweaking" of the matrix can result in a relatively well conditioned one. This process is simply that of adding a "small" constant to the diagonal term, which shifts the eigenvalues away from zero by that amount, hence quickly alleviating the ill conditioning. However, this also results in having a first-guess error correlation which has a Kronecker delta function at the origin. The result is that when the first-guess error is interpolated to the observation points, it spreads this additional term throughout the region. The effect of this perturbation must be assessed before it can be

concluded that the subsequent results are valid. Therefore, we first consider the process, and the effect of adding a constant to the diagonal of the covariance matrix.

Each realization of the process consists of the following steps, assuming the spatial correlation matrix has been previously factored to supply as input to the random number generator (I used GGNSM from the IMSL library). Normally distributed first-guess errors with the specified spatial correlation and standard deviation are generated. Independent, normally distributed errors with specified standard deviation are generated for the observation points. The first-guess error function is then interpolated to the observation points, and the first-guess minus observation error computed for the observation locations. Then the products of these errors are computed for each possible pair of observation locations.

This process is then repeated for a given number of realizations, and the average value of the product for each pair of stations computed. This results in the matrix (of order equal to the number of observation locations) of empirical covariances over the set of realizations. Only the upper triangular part is computed. The empirical standard deviation for each location is the square root of the corresponding diagonal term of the matrix, and the correlation matrix is obtained by dividing each row and column by the corresponding standard deviations. The entries in this matrix are the data plotted in parts (a) and (c) of Figs. A1-A4 as a function of distance between observation locations.

This data is then averaged over $.5^{o}$ intervals by simply taking an arithmetic average of the values in each interval $[.5(n-1),.5n)$ for n=1,.. . This is the data, plotted at the midpoints of the given intervals, in parts (b) and (d) of Figs. A1-A4.

As noted above, the correlation matrix tends to be ill conditioned in the case of interest. The following analysis shows that the simple expedient of adding a small term to the diagonal does not perturb the resulting empirical correlation matrix too much. Suppose that the desired isotropic spatial covariance function for the first guess errors is $\sigma_f^2 C(s)$ and the variance of the observation errors is σ_o^2. The covariance function to be simulated is

$$E[(I(e_f) - e_o)(p)(I(e_f) - e_o)(q)] = \sigma_f^2 C(s) + \sigma_o^2 \delta(s) ,$$

where $I(e_f)$ is the first-guess error function, obtained by interpolation (the errors of this process are relatively small for this case, and ignored) to the observation locations, e_o is the observation error function, $\delta(s)$ is the Kronecker delta function (zero except at s=0, where it is 1), and s is the distance between observation points p and q. Division by the variance yields the correlation, which for s>0 is

$$(A1) \quad R\, C(s) ,$$

where $R = \sigma_f^2/(\sigma_f^2 + \sigma_o^2)$.

Now, suppose the first-guess error, $\tilde{e}_f$, has spatial covariance $\sigma_f^2 C(s) + c^2 \delta(s)$. This first-guess error can be viewed as the sum of the previous errors and independent, uncorrelated errors at the grid points. Then, the interpolation of the first-

guess error gives the sum of the interpolation functions for the previous error (the interpolation assumed to be without error) and for the independent errors at the grid points, due to the additional diagonal term. The covariance function for linear combinations (obtained by interpolation to points p and q) of independent random variables, r_i, with variance c^2, is

$$E[(\sum_i b_i(p)r_i)(\sum_j b_j(q)r_j)] = c^2\sum_i b_i(p)b_i(q) = c^2B(p,q) \ .$$

This function is seen to be nonstationary, with variance $c^2B(p,p)$. Fortunately, the function B(p,q) is rather well behaved in our case. The interpolation is by piecewise bicubics, for which the coefficients are usually less than one, except in the boundary rectangles, where they may be slightly larger than one. In any case, the value of the B(p,q) lies between zero and 1.4, and is zero except when the points p and q are close enough together to use some of the same grid point values for the interpolation. This only happens when p and q are within about 15^o, and B(p,q) will be quite small unless they are in the same or adjacent rectangles of the grid.

Thus, the covariance function for the process is

$$E[I(\tilde{e}_f - e_o)(p)(\tilde{e}_f - e_o)(q)] = \sigma_f^2 C(s) + c^2B(p,q) + \sigma_o^2\delta(s) \ .$$

After division by the standard deviations at points p and q, the resulting correlation function, for s>0, is

$$(A2) \quad [C(s) + c^2B(p,q)]/(\sigma_f^2 + c^2B^*(p,q) + \sigma_o^2) \ ,$$

where $B^*(p,q)$ is the value which satisfies the equality

$$\sigma_f^2 + c^2 B^*(p,q) + \sigma_o^2 =$$
$$[(\sigma_f^2 + c^2 B(p,p) + \sigma_o^2)(\sigma_f^2 + c^2 B(q,q) + \sigma_o^2)]^{1/2} .$$

The value of $B^*(p,q)$ corresponds to a kind of geometric average of the two values $B(p,p)$ and $B(q,q)$ and lies between them, hence is bounded by the bound on $B(p,q)$.

The function in Eq. A2 must be compared with that given by A1. After some manipulation, it is possible to write the expression A2 as

(A3) $RC(s) - R\breve{c}^2[(RB^*(p,q)C(s)-B(p,q))/(1+\breve{c}^2 RB^*(p,q)]$,

where $\breve{c}^2 = c^2/\sigma_f^2$.

Thus the correlation functions for the two processes differ by the second term of Eq. A3. Since $B^*(p,q)$ and $B(p,q)$ are of reasonable magnitude, the effect is seen to be on the order of the relative amount added to the diagonal term, $\breve{c}^2$, which in the present case was about 0.0001 .

To check on the computational validity of the above, some simulations were run using $c^2 = 900$, a large value for the other parameter values, given in the next paragraph, and one that should affect the results significantly. The empirical correlation function should be diminished by about a factor of about $0.43C(s)$ for "large" distances, and less for small distances. This behavior was verified.

The above analysis allows the conclusion that adding a "small" amount to the diagonal of the correlation matrix will not seriously affect the empirical correlation data obtained. For purposes of the experiments reported on below, $c = 0.1$, with $\sigma_f = 30$, and $\sigma_o = 10$ for $R = .9$. The model correlation function

adopted was the six term Bessel function of section 4, with $c^2 = 0.01$ added to the diagonal for purposes of generating the first-guess error correlation matrix.

Part (a) of Figs. A1-A4 show the raw spatial correlation data for first-guess plus observation error for the separation between pairs of the 36 observation points, where 100 realizations of the process were averaged. Each figure corresponds to realizations with different initial seed numbers for the random number generator. Part (c) of the same figures show the corresponding data when 500 realizations were averaged, 400 more being done in addition to those of part (a). Parts (b) and (d) give the results after averaging the data of parts (a) and (c), respectively, over $.5^{\circ}$ intervals, along with a plot of the model correlation function.

Several comments are in order. The data of parts (a) and (b) (less the actual correlation plot) are reminiscent of that in previously mentioned papers in that the data is qualitatively similar, and is over about the same number of realizations, i.e., averages for one quarter at a given time of day would result in slightly fewer realizations. Given the much less scatter in part (c) and the far better agreement between the simulated data and the model correlation function in part (d), it is easy to conclude that it is possible that far more than 100 realizations are necessary to obtain a good estimate of the correlation function. Of course, there are many other variables which will tend to increase the scatter in any real data analog of part (a)

of the figures, among them anisotropy and nonstationarity of the first-guess error correlation and first-guess and observation error variances. The effect of this on the real data analog of part (b) is not easily discernible, and in any case will depend on the way the observation locations are distributed. In this context, the "out of place" points in part (d) of the figures, near distances of 11° and 16° may be due to the fact that far fewer observation point pairs happened to fall into that distance interval than for adjacent intervals. This phenomenon also accounts for the increasing scatter at greater distances, where there are few observation pairs so far apart. Although the scatter is less, the same phenomenon occurs at small distances, and lack of data at small distances makes accurate estimation of the function a problem, as was noted in section 4.

Figure Captions

Figure A1: (a) Scatter-plot of empirical correlation between first-guess minus observed values as a function of distance for 100 realizations using the MUS grid and observation point set. (b) Interval averaged scatterplot of the data in part (a) and the true correlation function for first-guess minus observed errors. (c) As in (a), but for an additional 400 realizations. (d) As in (b), but for the data in part (c).

Figure A2: Same as Fig. 1 for a different set of realizations.

Figure A3: Same as Fig. 1 for a different set of realizations.

Figure A4: Same as Fig. 1 for a different set of realizations.

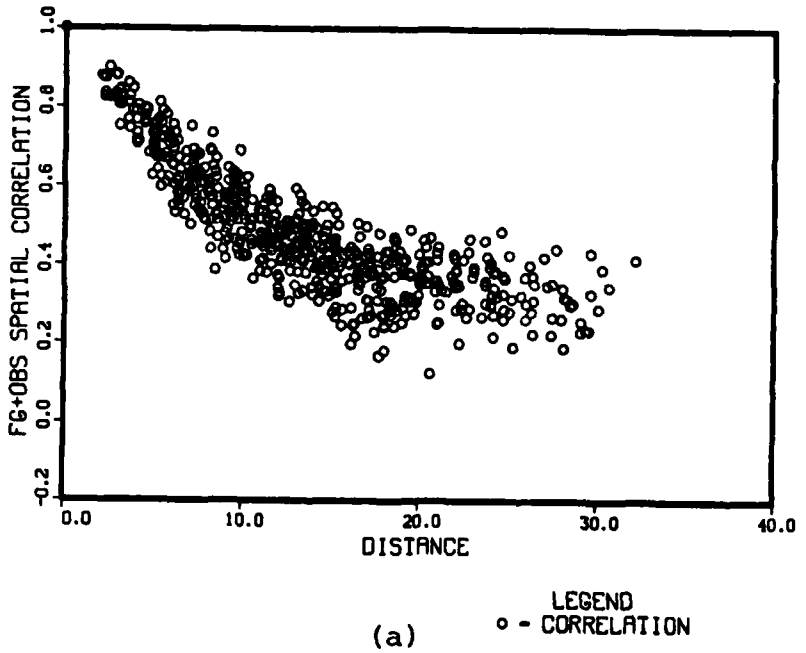
POINT-POINT CORRELATION PLOT
FG+OBS SPATIAL CORRELATION
1.0
0.8
0.6
0.4
0.2
0.0
-0.2
0.0
10.0
20.0
30.0
40.0
DISTANCE
LEGEND
o - CORRELATION

(a)

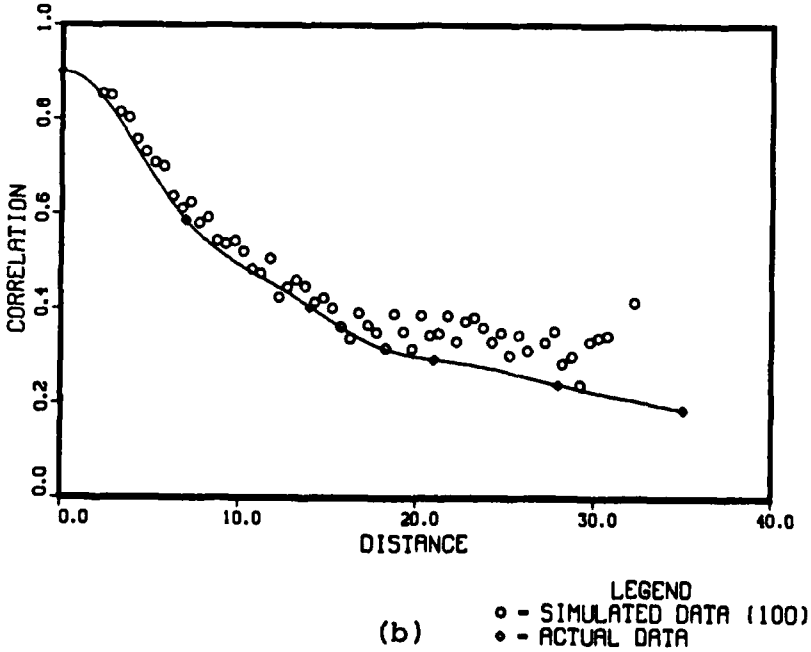
6 TERM BESSEL DATA
CORRELATION
1.0
0.8
0.6
0.4
0.2
0.0
0.0
10.0
20.0
30.0
40.0
DISTANCE
LEGEND
o - SIMULATED DATA (100)
• - ACTUAL DATA

(b)

FIGURE A1

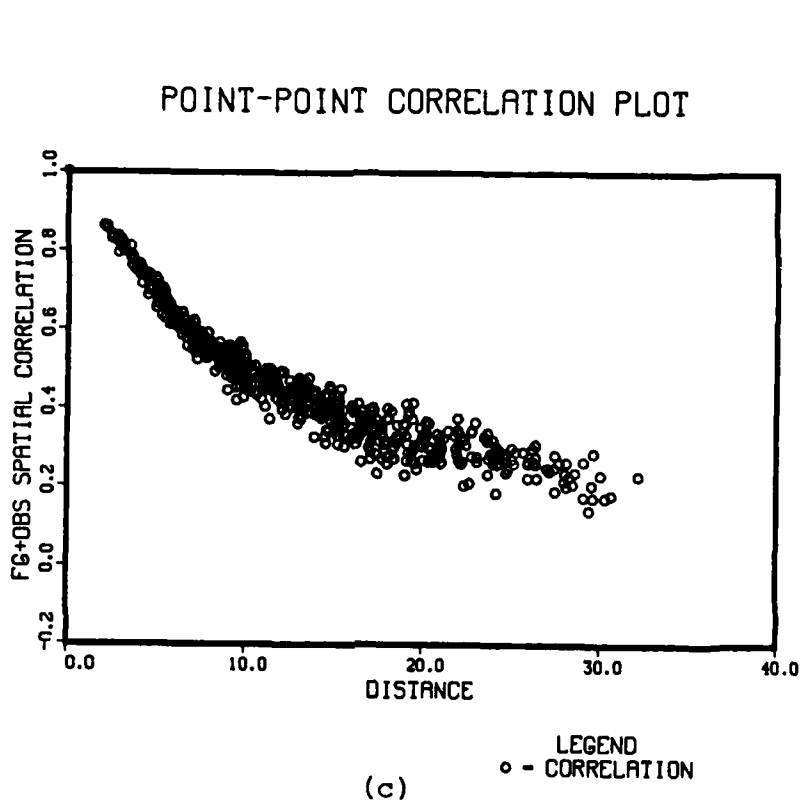
POINT-POINT CORRELATION PLOT
FG+OBS SPATIAL CORRELATION
1.0
0.8
0.6
0.4
0.2
0.0
-0.2
0.0
10.0
20.0
30.0
40.0
DISTANCE
LEGEND
o - CORRELATION

(c)

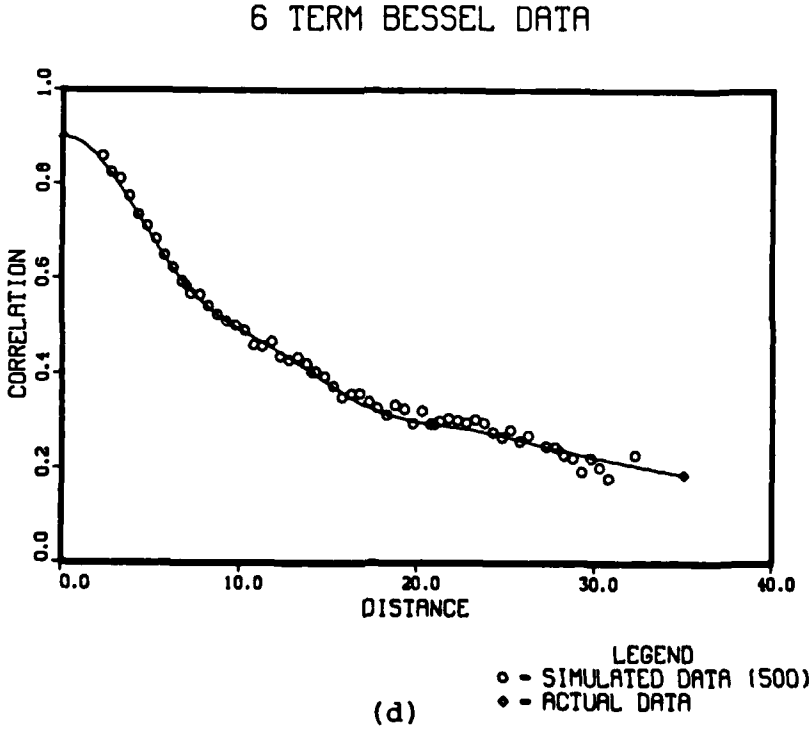
6 TERM BESSEL DATA
CORRELATION
1.0
0.8
0.6
0.4
0.2
0.0
0.0
10.0
20.0
30.0
40.0
DISTANCE
LEGEND
o - SIMULATED DATA (500)
◆ - ACTUAL DATA

(d)

FIGURE A1

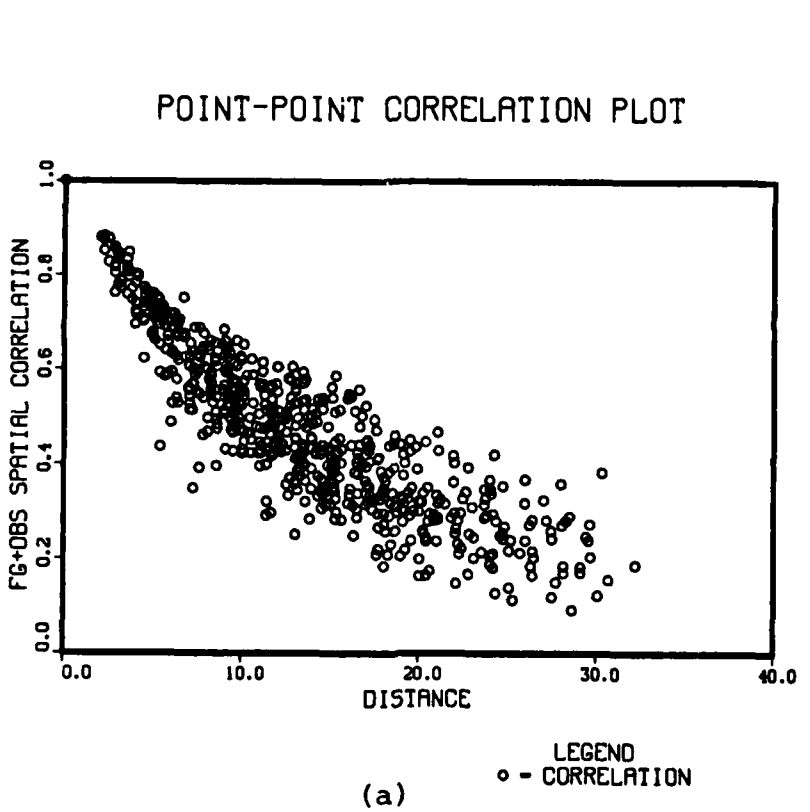
POINT-POINT CORRELATION PLOT
FG+OBS SPATIAL CORRELATION
0.0
0.2
0.4
0.6
0.8
1.0
0.0
10.0
20.0
30.0
40.0
DISTANCE
LEGEND
o - CORRELATION

(a)

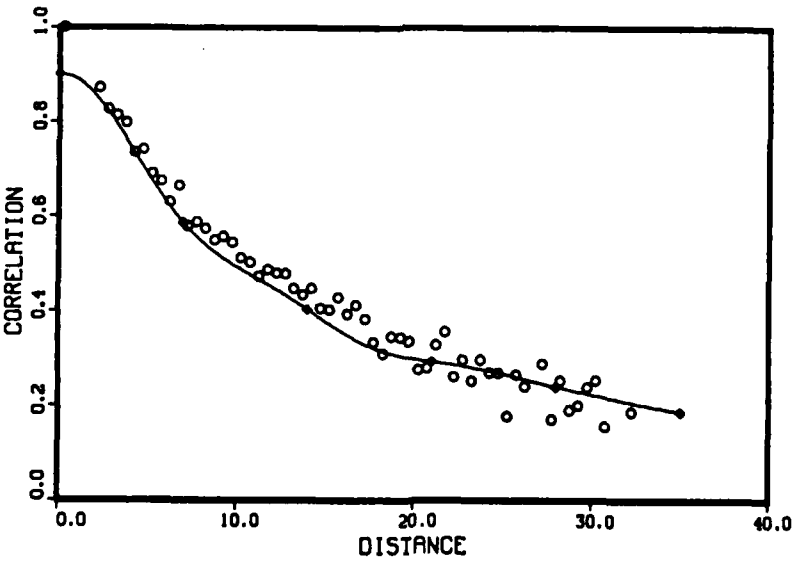
6 TERM BESSEL DATA
CORRELATION
0.0
0.2
0.4
0.6
0.8
1.0
0.0
10.0
20.0
30.0
40.0
DISTANCE
LEGEND
o - SIMULATED DATA
• - ACTUAL DATA

(b)

FIGURE A2

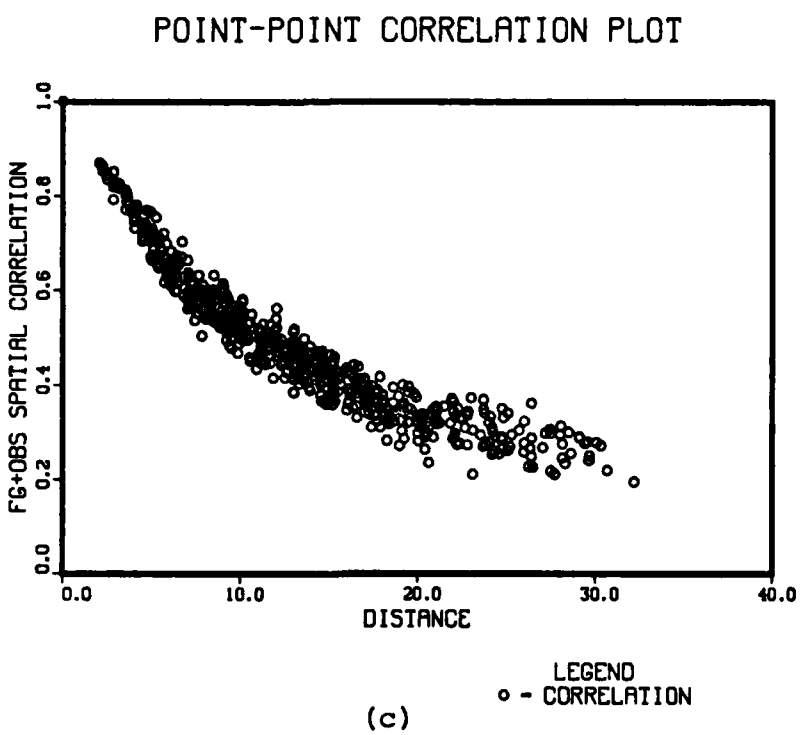
POINT-POINT CORRELATION PLOT
FG+OBS SPATIAL CORRELATION
0.0
0.2
0.4
0.6
0.8
1.0
0.0
10.0
20.0
30.0
40.0
DISTANCE
LEGEND
o - CORRELATION

(c)

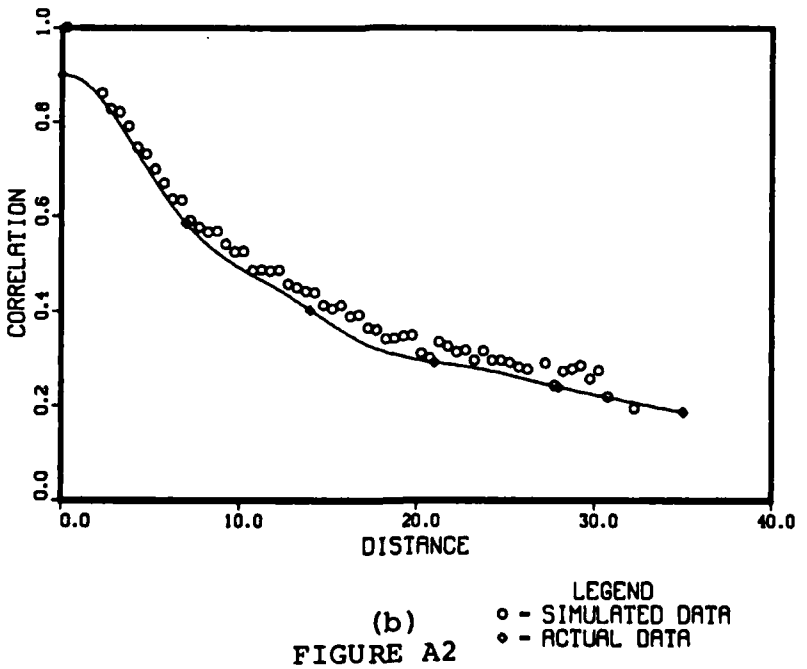
6 TERM BESSEL DATA
CORRELATION
0.0
0.2
0.4
0.6
0.8
1.0
0.0
10.0
20.0
30.0
40.0
DISTANCE
LEGEND
o - SIMULATED DATA
◇ - ACTUAL DATA

(b)

FIGURE A2

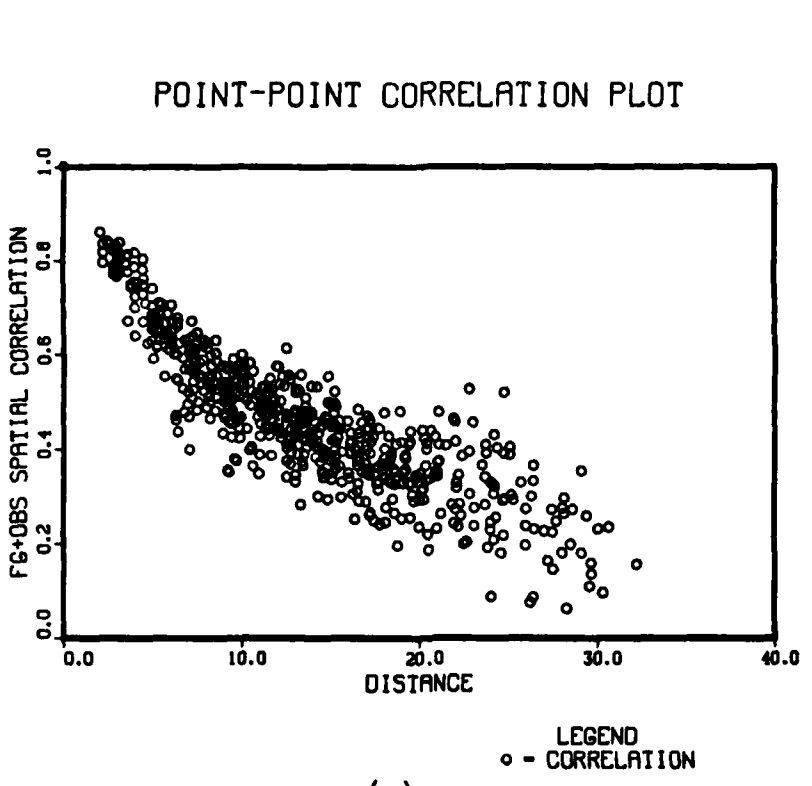
POINT-POINT CORRELATION PLOT
FG+OBS SPATIAL CORRELATION
0.0
0.2
0.4
0.6
0.8
1.0
0.0
10.0
20.0
30.0
40.0
DISTANCE
LEGEND
o - CORRELATION

(a)

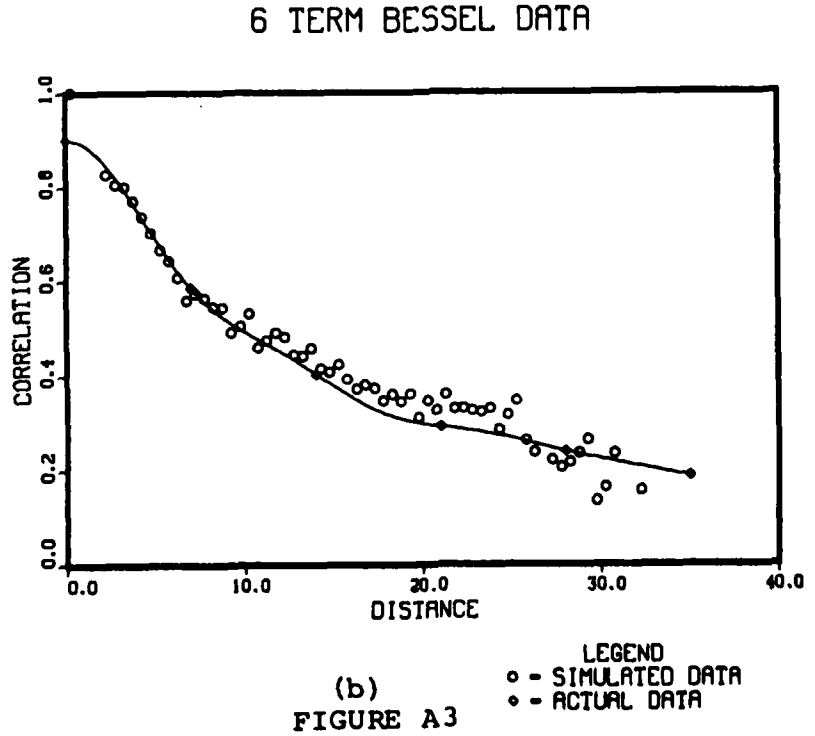
6 TERM BESSEL DATA
CORRELATION
0.0
0.2
0.4
0.6
0.8
1.0
0.0
10.0
20.0
30.0
40.0
DISTANCE
LEGEND
o - SIMULATED DATA
◇ - ACTUAL DATA

(b)

FIGURE A3

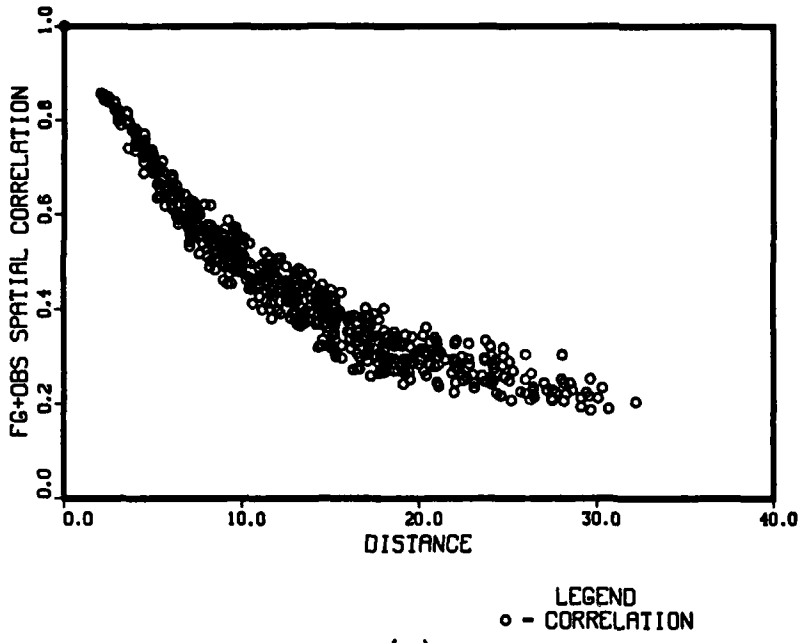
POINT-POINT CORRELATION PLOT
FG+OBS SPATIAL CORRELATION
0.0
0.2
0.4
0.6
0.8
1.0
0.0
10.0
20.0
30.0
40.0
DISTANCE
LEGEND
o - CORRELATION

(c)

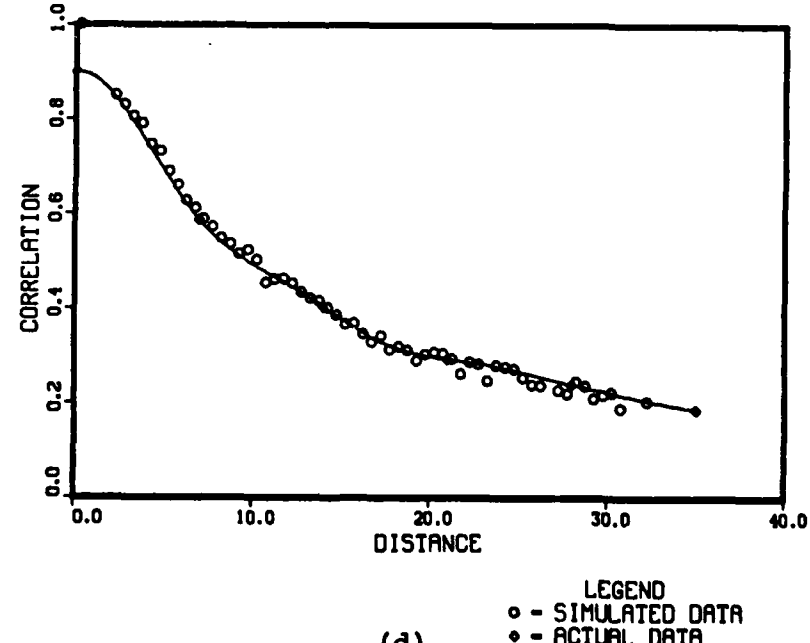
6 TERM BESSEL DATA
CORRELATION
0.0
0.2
0.4
0.6
0.8
1.0
0.0
10.0
20.0
30.0
40.0
DISTANCE
LEGEND
o - SIMULATED DATA
◆ - ACTUAL DATA

(d)

FIGURE A3

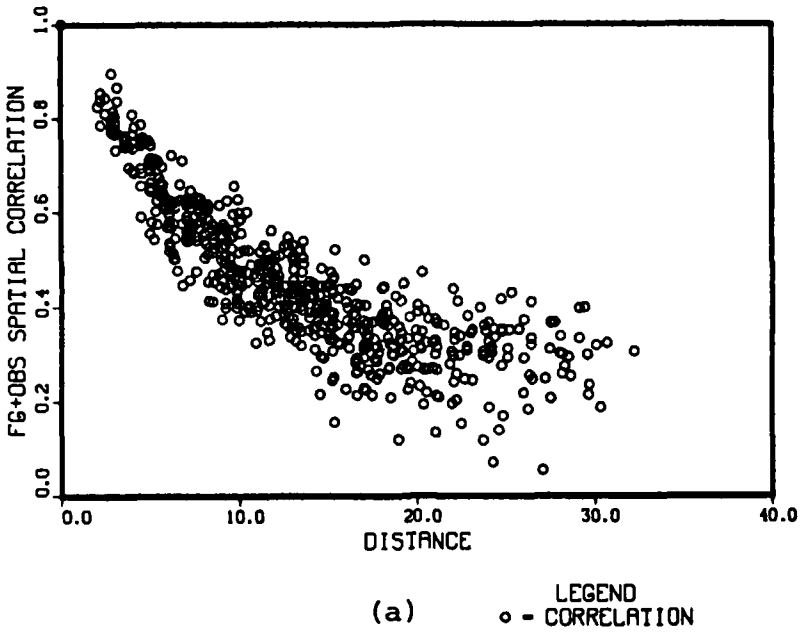
POINT-POINT CORRELATION PLOT
FG+OBS SPATIAL CORRELATION
0.0
0.2
0.4
0.6
0.8
1.0
0.0
10.0
20.0
30.0
40.0
DISTANCE
LEGEND
o - CORRELATION

(a)

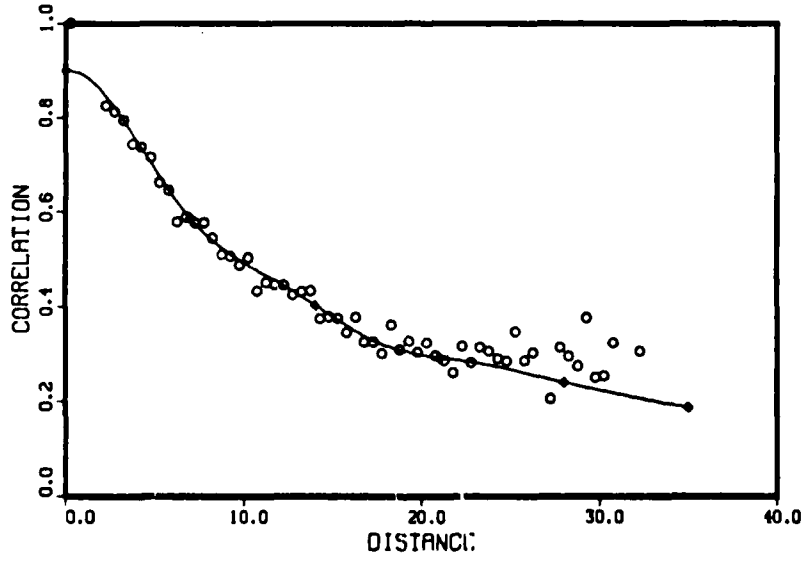
6 TERM BESSEL DATA
CORRELATION
0.0
0.2
0.4
0.6
0.8
1.0
0.0
10.0
20.0
30.0
40.0
DISTANCE
LEGEND
o - SIMULATED DATA
◇ - ACTUAL DATA

(b)

FIGURE A4

POINT-POINT CORRELATION PLOT

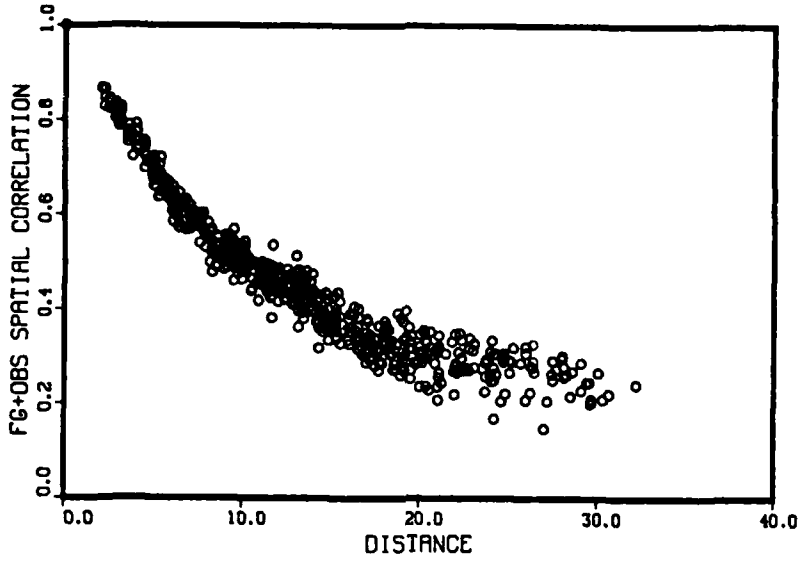

(c)

LEGEND
o - CORRELATION

6 TERM BESSEL DATA

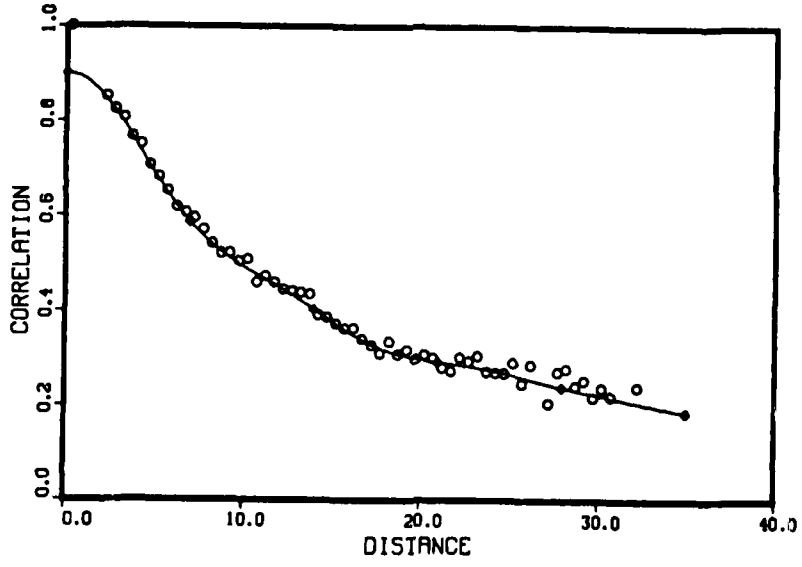

(d)

LEGEND
o - SIMULATED DATA
◇ - ACTUAL DATA

FIGURE A4

INITIAL DISTRIBUTION LIST

ASST. FOR ENV. SCIENCES
ASST. SEC. OF THE NAVY (R&D)
ROOM 5E731, THE PENTAGON
WASHINGTON, DC 20350

OFFICE OF NAVAL RESEARCH
CODE 422AT
ARLINGTON, VA 22217

COMMANDING OFFICER
FLENUMOCEANCEN
MONTEREY, CA 93943

NAVAL POSTGRADUATE SCHOOL
METEOROLOGY DEPT.
MONTEREY, CA 93943

LIBRARY (2)
NAVAL POSTGRADUATE SCHOOL
MONTEREY, CA 93943

COMMANDER
NAVAIRSYSCOM (AIR-330)
WASHINGTON, DC 20361

USAFETAC/TS
SCOTT AFB, IL 62225

AFGWC/DAPL
OFFUTT AFB, NE 68113

AFGL/OPI
HANSCOM AFB, MA 01731

COMMANDER & DIRECTOR
ATTN: DELAS-D
U.S. ARMY ATMOS. SCI. LAB
WHITE SAND MISSILE RANGE
WHITE SANDS, NM 88002

NOAA-NESDIS LIAISON
ATTN: CODE SC2
NASA-JOHNSON SPACE CENTER
HOUSTON, TX 77058

CHIEF OF NAVAL RESEARCH (2)
LIBRARY SERVICES, CODE 784
BALLSTON TOWER #1
800 QUINCY ST.
ARLINGTON, VA 22217

COMMANDING OFFICER
NORDA
NSTL, MS 39529

SUPERINTENDENT
LIBRARY REPORTS
U. S. NAVAL ACADEMY
ANNAPOLIS, MD 21402

NAVAL POSTGRADUATE SCHOOL
OCEANOGRAPHY DEPT.
MONTEREY, CA 93943

COMMANDER (2)
NAVAIRSYSCOM
ATTN: LIBRARY (AIR-7226)
WASHINGTON, DC 20361

COMMANDER
NAVOCEANSYSCEN
DR. J. RICHTER, CODE 532
SAN DIEGO, CA 92152

SUPERINTENDENT
ATTN: USAFA (DEG)
COLORADO SPRINGS, CO 80840

AFGL/LY
HANSCOM AFB, MA 01731

OFFICER IN CHARGE
SERVICE SCHOOL COMMAND
DET. CHANUTE/STOP 62
CHANUTE AFB, IL 61868

DIRECTOR (2)
DEFENSE TECH. INFORMATION
CENTER, CAMERON STATION
ALEXANDRIA, VA 22314

DIRECTOR
NATIONAL METEORO. CENTER
NWS, NOAA
WWB W32, RM 204
WASHINGTON, DC 20233

ACQUISITIONS SECT. IRDB-DB23
LIBRARY & INFO. SERV., NOAA
6009 EXECUTIVE BLVD.
ROCKVILLE, MD 20852

NATIONAL WEATHER SERVICE
WORLD WEATHER BLDG., RM 307
5200 AUTH ROAD
CAMP SPRINGS, MD 20023

DIRECTOR
GEOPHYS. FLUID DYNAMICS LAB
NOAA, PRINCETON UNIVERSITY
P.O. BOX 308
PRINCETON, NJ 08540

LABORATORY FOR ATMOS. SCI.
NASA GODDARD SPACE FLIGHT CEN.
GREENBELT, MD 20771

COLORADO STATE UNIVERSITY
ATMOSPHERIC SCIENCES DEPT.
ATTN; DR. WILLIAM GRAY
FORT COLLINS, CO 80523

CHAIRMAN, METEOROLOGY DEPT.
UNIVERSITY OF OKLAHOMA
NORMAN, OK 73069

COLORADO STATE UNIVERSITY
ATMOSPHERIC SCIENCES DEPT.
ATTN; LIBRARIAN
FT. COLLINS, CO 80523

UNIVERSITY OF WASHINGTON
ATMOSPHERIC SCIENCES DEPT.
SEATTLE, WA 98195

FLORIDA STATE UNIVERSITY
ENVIRONMENTAL SCIENCES DEPT.
TALLAHASSEE, FL 32306

DIRECTOR
COASTAL STUDIES INSTITUTE
LOUISIANA STATE UNIVERSITY
ATTN: O. HUH
BATON ROUGE, LA 70803

DIRECTOR
OFFICER OF PROGRAMS RX3
NOAA RESEARCH LAB
BOULDER, CO 80302

DIRECTOR
NATIONAL SEVERE STORMS LAB
1313 HALLEY CIRCLE
NORMAN, OK 73069

DIRECTOR
TECHNIQUES DEVELOPMENT LAB
GRAMAX BLDG.
8060 13TH ST.
SILVER SPRING, MD 20910

EXECUTIVE SECRETARY, CAO
SUBCOMMITTEE ON ATMOS. SCI.
NATIONAL SCIENCE FOUNDATION
RM. 510, 1800 G. STREET, NW
WASHINGTON, DC 20550

ATMOSPHERIC SCIENCES DEPT.
UCLA
405 HILGARD AVE.
LOS ANGELES, CA 90024

CHAIRMAN, METEOROLOGY DEPT.
CALIFORNIA STATE UNIVERSITY
SAN JOSE, CA 95192

NATIONAL CENTER FOR ATMOS.
RSCH., LIBRARY ACQUISITIONS
P.O. BOX 3000
BOULDER, CO 80302

CHAIRMAN, METEOROLOGY DEPT.
PENNSYLVANIA STATE UNIVERSITY
503 DEIKE BLDG.
UNIVERSITY PARK, PA 16802

UNIVERSITY OF HAWAII
METEOROLOGY DEPT.
2525 CORREA ROAD
HONOLULU, HI 96822

ATMOSPHERIC SCIENCES DEPT.
OREGON STATE UNIVERSITY
CORVALLIS, OR 97331

UNIVERSITY OF MARYLAND
METEOROLOGY DEPT.
COLLEGE PARK, MD 20742

CHAIRMAN
ATMOS. SCIENCES DEPT.
UNIVERSITY OF VIRGINIA
CHARLOTTESVILLE, VA 22903

CHAIRMAN
METEOROLOGY DEPT.
MASSACHUSETTS INSTITUTE OF TECHNOLOGY
CAMBRIDGE, MA 02139

CHAIRMAN, METEOROLOGY DEPT.
UNIVERSITY OF UTAH
SALT LAKE CITY, UT 84112

ATMOSPHERIC SCIENCES CENTER
DESERT RESEARCH INSTITUTE
P.O. BOX 60220
RENO, NV 89506

ATMOSPHERIC SCI. RSCH. CENTER
NEW YORK STATE UNIVERSITY
1400 WASHINGTON AVE.
ALBANY, NY 12222

SYSTEMS & APPLIED SCI. CORP.
ATTN: LIBRARY, SUITE 500
6811 KENILWORTH AVE.
RIVERDALE, MD 20840

CENTER FOR ENV. & MAN, INC.
RESEARCH LIBRARY
275 WINDSOR ST.
HARTFORD, CT 06120

METEOROLOGY RESEARCH, INC.
464 W. WOODBURY RD.
ALTADENA, CA 91001

METEOROLOGY INTL., INC.
P.O. BOX 22920
CARMEL, CA 93922

CONTROL DATA CORP.
METEOROLOGY DEPT. RSCH. DIV.
2800 E. OLD SHAKOPEE RD.
BOX 1249
MINNEAPOLIS, MN 55440

SCIENCE APPLICATIONS, INC.
205 MONTECITO AVENUE
MONTEREY, CA 93940

OCEAN DATA SYSTEMS, INC.
2460 GARDEN ROAD
MONTEREY, CA 93940

EUROPEAN CENTRE FOR MEDIUM RANGE WEATHER FORECASTS
SHINFIELD PARK, READING
BERKSHIRE RG29AX, ENGLAND

DEAN OF RESEARCH
CODE 012
NAVAL POSTGRADUATE SCHOOL
MONTEREY, CA 93943

DEPT. OF MATHEMATICS
NAVAL POSTGRADUATE SCHOOL
MONTEREY, CA 93943

PROFESSOR H. FREDRICKSEN
CHAIRMAN, DEPT OF MATHEMATICS
NAVAL POSTGRADUATE SCHOOL
MONTEREY, CA 93943

PROFESSOR R. FRANKE, 53Fe
DEPT. OF MATHEMATICS (10)
NAVAL POSTGRADUATE SCHOOL
MONTEREY, CA 93943

DR. RICHARD LAU
OFFICE OF NAVAL RESEARCH
800 QUINCY ST.
ARLINGTON, VA 22217

PROFESSOR R.E. BARNHILL
DEPT. OF COMPUTER SCIENCE
ARIZONA STATE UNIVERSITY
TEMPE, AZ 85287

PROFESSOR G.M. NIELSON
DEPT. OF COMPUTER SCIENCE
ARIZONA STATE UNIVERSITY
TEMPE, AZ 85287

LIBRARY, FLEET NUMERICAL (2)
OCEANOGRAPHY CENTER
MONTEREY, CA 93943

DR. EDWARD BARKER (5)
NAVAL ENVIRONMENTAL PREDICTION
RESEARCH FACILITY
MONTEREY, CA 93943

DR. THOMAS ROSMOND
NAVAL ENVIRONMENTAL PREDICTION
RESEARCH FACILITY
MONTEREY, CA 93943

PROFESSOR W.J. GORDON
CENTER FOR SCIENTIFIC
COMPUTATION & INTERACTIVE
GRAPHICS
DREXEL UNIVERSITY
PHILADELPHIA, PA 19104

PROFESSOR GRACE WAHBA
DEPARTMENT OF STATISTICS
UNIVERSITY OF WISCONSIN
MADISON, WI 53705

DR. H. JEAN THIEBAUX
NATIONAL METEOROLOGICAL CENTER
W/NMC2
WWB
WASHINGTON, DC 20233

DR. R.S. SEAMAN
AUSTRALIAN NUMERICAL
METEOROLOGY RESEARCH CENTRE
P.O. BOX 5089AA
MELBOURNE, VICTORIA,
AUSTRALIA, 3001

PROFESSOR PETER ALFELD
DEPARTMENT OF MATHEMATICS
UNIVERSITY OF UTAH
SALT LAKE CITY, UT 84112

PROFESSOR MARK E. HAWLEY
DEPARTMENT OF ENVIRONMENTAL
SCIENCES
UNIVERSITY OF VIRGINIA
CHARLOTTESVILLE, VA 22903

DR. LAWRENCE BREAKER
DEPARTMENT OF OCEANOGRAPHY
NAVAL POSTGRADUATE SCHOOL
MONTEREY, CA 93943

PROFESSOR JAMES J. O'BRIEN
DEPARTMENT OF METEOROLOGY
THE FLORIDA STATE UNIVERSITY
TALLAHASSEE, FLORIDA 32306

MR. ROSS HOFFMAN
ATMOSPHERIC AND ENVIRONMENTAL
RESEARCH, INC.
840 MEMORIAL DRIVE
CAMBRIDGE, MA 02139

DR. JAMES GOERSS
NAVAL ENVIRONMENTAL PREDICTION
RESEARCH FACILITY
MONTEREY, CA 93943

1STLT KEN GALLUPPI
USAFETAC/DNO
SCOTT AFB, IL 62225-5438

DR. LICIA LENARDUZZI
IAMI
VIA CICOGNARA 7
20129 MILANO
ITALIA

DR. PAUL F. TWITCHELL
OFFICE OF NAVAL RESEARCH
800 QUINCY ST.
ARLINGTON, VA 22217

PROF. GORDON E. LATTA
DEPT. OF MATHEMATICS
NAVAL POSTGRADUATE SCHOOL
MONTEREY, CA 93943

END

1-87

DTIC